October 21, 2012 FERMILAB-TM-2541-PPD

The muon certification procedure of the D0 experiment in Run II

Oleg Brandt[a,b], SungWoong Cho[c], Michael Cooke[a], Michael Eads[d], Dave Hedin[e], Jeong Ku Lim[c], Sung Park[c], Angelo Santos[f], Jadranka Sekaric[g], Boris Tuchming[h], Yuriy Yatsunenko[i], SungWoo Youn[a]

for the DØ Muon Algorithms and Identification group.

[a] Fermilab
[b] Göttingen University
[c] Korea University
[d] Nebraska University
[e] Northern Illinois University
[f] Universidade Estadual Paulista
[g] Kansas University
[h] IRFU/SPP, CEA-Saclay, France
[i] JINR

Abstract

This technical memo note describes the procedures used by the D0 experiment at the Fermilab Tevatron $p\bar{p}$ Collider to determine the identification and reconstruction efficiencies for specific muon selection criteria for both data and Monte Carlo simulation. Dedicated corrections for the muons satisfying these criteria are derived, thus certifying them to be used in physics analyses at D0. The results of the efficiencies of certified muons are presented for a sub-sample of 4.2 fb^{-1} collected by the D0 experiment. The experimental techniques and procedures employed here are identical to those used for the full 9.7 fb^{-1} dataset.

Acknowledgement

Operated by Fermi Research Alliance, LLC under Contract No. De-AC02-07CH11359 with the United States Department of Energy.

Contents

1 Introduction

The DØ detector is capable of identifying muons using three independent subsystems:

- The three-layer muon detector system with its toroid magnet covers more than 90% of the angular acceptance up to a pseudorapidity $|\eta| = 2$. It provides an unambiguous muon identification and, if a track segment can be reconstructed, a momentum measurement. A muon identified on the basis of the information provided by the muon detector is referred to as a **"local muon"**.

- The central tracking system (consisting of the Silicon Micro-strip Tracker – SMT – and the Central Fibre Tracker – CFT) provides an accurate momentum resolution and is highly efficient at finding muon tracks in the entire angular acceptance of the muon detector. A local muon that is successfully matched with a central track is called a **"central track-matched muon"**.

- A third independent muon confirmation can be obtained with the MIP signature in the calorimeter. The capability to identify muons using the calorimeter is called "Muon Tracking in the Calorimeter" or **"MTC"**. The current MTC algorithm has a typical efficiency of $\approx 50\%$, far less efficient than the other muon signatures. Currently, MTC muons are not officially certified.

This document describes the certified Muon Identification (MuonID) definitions to be used with the Summer 2009 Extended dataset corresponding to an integrated luminosity of 4.2 fb^{-1}. This dataset was reconstructed with version `p20` of the DØ event reconstruction software and passed through the `p21.18.00` version of `d0correct`. The corresponding certification of the `p17` RunIIa and `p20` Moriond 2008 datasets corresponding to 1 fb^{-1} and 2.5 fb^{-1} can be found in Ref. [1] and [2], respectively.

The experimental techniques and procedures used to determine the identification and reconstruction efficiencies of prompt muons presented in this technical memo note are identical to those used for the full 9.7 fb^{-1} dataset collected by the D0 experiment during Run II of Fermilab's Tevatron $p\bar{p}$ Collider, and thus of general nature.

Over a period of more than half a year in 2009 and 2010, a substantial amount of work has gone into a detailed understanding of the performance of the DØ detector for the identification and reconstruction of prompt muons, improving the identification efficiency, and reducing the luminosity dependence. This necessitated the introduction of new muon track quality and isolation definitions, and new experimental techniques such as the parametrization of data/MC Scale Factors (SFs) in terms of luminosity. The certification procedure was also revised with some requirements modified to reduce background contributions and added to the ntuple to study their systematic impact.

The samples used to derive the data-MC corrections are described in Section 4. The new procedure to account for a different luminosity profile in the certification samples (both data and MC) and a typical muon-based skim like `2MUhighpt` is introduced in Section 5. The efficiencies for muon and track identification as well as isolation efficiencies for prompt leptons are discussed in Sections 6, 7, 8, respectively, alongside with the estimation of some systematic uncertainties.

Some studies on muon performance done during 2009 are not included in this note. The "local" muon-system-only momentum resolution was investigated in Ref. [3]. The understanding of the central tracking resolution and how to add additional smearing to MC events to reproduce what is observed in the data is described in Ref. [4]. The momentum resolution work for the Summer 2009 Extended dataset of 4.2 fb^{-1} and other datasets was concluded in 2011 and is documented in Ref. [5]. Also, there has not been any additional work on muon backgrounds; for that subject refer to the `p17` note Ref. [1] or an earlier note on punchthroughs Ref. [6].

2 Summary: Major Changes with Respect to p17

This Section aims at presenting a brief summary of what the user familiar with muon analysis with `p17` and the previous version of `p20` muon identification algorithms should know when analyzing the Summer 2009 Extended dataset (with `p21 d0correct`). For the differences between the Moriond 2008 and Run IIa `p17` dataset please refer to [2], for the differences between `p17` and p14 to [1].

Please note that, like in the previous certification rounds, the data/MC Scale Factors (SFs) for offline muon reconstruction and triggers are valid *only* for high p_{T} muons ($p_{\text{T}} > 20\,\text{GeV}$), whereas tracking and isolation SFs are valid down to 15 GeV. There are plans to reduce this threshold to 15 GeV for triggers as well.

2.1 Improvements at the Offline Reconstruction Level

- The muon chunk array size, previously fixed to 100 muons (including nseg=0 muons), is now dynamic (as of `p20.16.07`)

2.2 Changes in Muon and Track Identification, as well as Isolation

- The muID definitions of loose and medium remain the same as the 2008 `p20` note which includes the change to the nseg=3 criteria in the central region which dropped the requirement of a BC-layer scintillator.

- The relaxation of the cosmics timing cut to 10 ns/10 ns/13 ns from 10 ns/10 ns/10 ns in layers A/B/C, resulting in an efficiency increase of about $^1/_2\%$, has been studied but not implemented. However it may be implemented in the next certification round due to the need to re-skim.

- The cosmics timing efficiency is included in the efficiency of the muID categories loose, medium, and mediumnseg3. We will now also include efficiencies without the timing cut in new categories looseNCV, mediumNCV, and mediumnseg3NCV.

- For muons matched to central track, the track quality definitions have been made more robust against high luminosity effects and fake tracks, as detailed in Section 7 and summarized in Subsection 3.3. The new track quality definitions are named: trackloose, tracknewmedium, trackmedium, and tracktight.

- The isolation requirements for muons in order to reject non-prompt muons from e.g. heavy flavour decays has been adopted to cope with the high luminosity requirements. New, even more luminosity-robust isolation requirements have been introduced: TrkLooseScaled, TrkTightScaled, TrkLoose, and TrkLoose. All this is described in Section 8 and summarized in Subsection 3.4;
- various minor bug fixes and updates.

2.3 Changes in the Muon Certification Procedure

There have been many adaptations of the `wzreco`, `muo_cert`, `muid_eff` packages. For `wzreco` and `muo_cert`, rather then cutting on a parameter in the `wzreco` dimuon selection, some quantities are now being saved on the ntuple so that studies can be made. In addition some bugs were fixed. The major changes are:

- An isolation cut is added to the probe for the track_tree selection
- The tracking and isolation SPC files produced in `muid_eff` have a luminosity dependence
- Efficiencies are weighted to the luminosity profile of the `2MUhighpt` skim

2.4 CAFe Features

The following CAFe features have been implemented:

- In the `MuonSelector` [7] the new definition of track and isolation quality cuts has been implemented, alongside with the "old" track quality definitions used in `p17` [1];
- Data/MC Scale Factors (SFs) applied using the `caf_eff_utils` [8] package can be parametrised in terms of luminosity $\mathscr{L}$ and the absolute pseudorapidity measured at the outer boundary of the CFT η_{CFT};
- It is possible to factorise the efficiency SFs in two sets of (uncorrelated) variables preserving overall normalisation. Now e.g. the tracking efficiency SFs are parametrised in $\eta_{\mathrm{CFT}} \times z_0 \oplus |\eta_{\mathrm{CFT}}| \times \mathscr{L}$;
- Possibility to model trigger efficiency[8, 9].

2.5 V + jets CAFe Features

The standard V + jets data/MC correction procedure has been improved:

- in the `caf_eff_utils` [8] package we now correct for data/MC efficiency differences at five (up to now only 4) stages:
  - for muon identification efficiency parametrised in $\eta \times \varphi$ (1 step);
  - for tracking efficiency parametrised in $\eta_{\mathrm{CFT}} \times z_0 \oplus |\eta_{\mathrm{CFT}}| \times \mathscr{L}$ (i.e. 2 steps);
  - for isolation efficiency of prompt muons: for $\Delta R(\mu, \text{closest jet}) > 0.5$ parametrised in $|\eta_{\mathrm{CFT}}| \times \mathscr{L}$ (1 step), for posterior isolation in $|\eta_{\mathrm{CFT}}| \times p_{\mathrm{T}} \times \Delta R$ (1 step);

3 Object Definitions

3.1 The New Muon Quality Definitions

Reconstructed muon candidates are classified using two parameters: muon *type* and muon *quality*. The *type* of muon is given by the parameter nseg. A positive value of nseg indicates that the muon reconstructed in the muon system ("local muon") was matched to a track in the central tracking system. A negative value of nseg tells that the local muon could not be matched to a central track. The absolute value |nseg| = 1, 2, or 3 respectively indicates that the local muon is made up of A-layer only hits, B or C-layer only hits (outside the toroid), or both A- and B- or C-layers hits. The different muon types with their respective values of nseg are listed in Table 1. Additional information about the various muon types can be found in [10].

nseg	**Muon Type**	**Central track matching algorithm**	**MTC matching criterion**
3	Central track + local muon track (A and BC layer)	Muon to central if local muon track fit converged. Central to muon otherwise	$\Delta\eta$, $\Delta\phi$ between MTC and central track extrapolated to calorimeter
2	Central track + BC only	central to muon	as above
1	Central track + A only	central to muon	as above
0	Central track + muon hit or central track + MTC	central to muon central to calorimeter	as above
-1	A segment only	no match	$\Delta\eta$, $\Delta\phi$ between MTC and and A-layer segment
-2	BC segment only	no match	$\Delta\eta$, $\Delta\phi$ between MTC and and BC-layer segment
-3	local muon track (A + BC)	no match	$\Delta\eta$, $\Delta\phi$ between MTC and local muon track at A-layer if fit converged or else A-segment position

Table 1: Overview of the different muon types.

The classification according to muon type, and the underlying muon reconstruction algorithm did not change since p14. The second parameter used to classify muons is the *quality*. The muon quality can be "loose", "medium" or "tight"[1]. The tight definition has remained

[1]Here, we follow the exact quality definition names used in the caf_util package and the vjets_cafe

unchanged since p10; however the certification procedure in p17 and p20 does not produce efficiencies for tight, which is not used within DØ to our knowledge. The medium and loose efficiencies were not changed since p17 (cf. Ref [1]). However, the medium definition for the nseg=3 type only (referred to as mediumnseg3) was changed for p20.

The definitions for medium and loose for p20 are given below (the definition for tight can be found in Ref. [1]):

- **|nseg|=3 medium/loose muons**
  An |nseg| = 3 muon is medium (i.e. mediumnseg3) if it has:
  - at least two A layer wire hits;
  - at least one A layer scintillator hit;
  - at least two BC layer wire hits;
  - at least one BC scintillator hit (except for central muons where this requirement is dropped).

  An |nseg| = 3 loose muon is defined as a mediumnseg3 muon but allowing one of the above tests to fail, with the A wire and scintillator requirement treated as one test and requiring always at least one scintillator hit.

- **nseg=+2 loose/medium muons**
  Muons with |nseg| < 3 can only be loose or medium if they are matched to a central track. nseg=2 muons are muons with a BC segment matched with a central track. loose requires:
  - at least one BC layer scintillator hit;
  - at least two BC layer wire hits.

  An nseg=2 muon is defined as medium if it fulfils the above requirements and if it is located in the bottom part of the detector (octant 5 and 6 with $|\eta^{\text{detector}}|$ <1.6).

- **nseg=+1 loose/medium muons**
  Muons with nseg=1 are muons with an A segment matched with a central track. An nseg=1 muon is loose if it has:
  - at least one scintillator hit;
  - at least two A layer wire hits.

  An nseg=1 muon is defined as medium if it fulfils the above requirements and if it is located in the bottom part of the detector (octant 5 and 6 with $|\eta^{\text{detector}}|$ <1.6). Low momentum nseg=1 muons are also defined as medium. A nseg=1 muon is qualified as low momentum muon if its probability to reach the BC layer is less than 0.7.

framework.

3.2 Cosmic Veto

This veto consists in rejecting cosmic muons using the scintillator hit times (when information is available):

- |A-layer time| < 10 ns
- |B-layer time| < 10 ns
- |C-layer time| < 10 ns

The efficiency of this is about 98.3%. It is worthwhile to notice that the trackloose, trackmedium and tracktight tracking criteria have *dca* cuts which also suppress cosmic muons. The inefficiency associated with this timing cut is included in the efficiencies for the muon identification criteria loose, medium and mediumnseg3. The efficiencies without the timing cuts are given in looseNCV, mediumNCV, and mediumnseg3NCV. Ref. [11] shows the efficiency and the cosmic ray muon rejection versus different timing cuts.

3.3 The New Track Quality Definitions

To control the purity of muons matched to central track, four operating points for track identification and reconstruction have been defined. They rely on the following track characteristics:

- number of hits either in the SMT or CFT system;
- χ^2 per degrees of freedom of the central track fit;
- transverse impact parameter (distance of closest approach in (x, y)) with respect to the beamline.

The `p17` track quality definitions are the following[2]:

- **trackloose track**
  A track is trackloose if $|dca| < 0.2$ cm. If the track has a SMT hit the cut is tightened to $|dca| < 0.02$ cm. Note that, for muons from Z boson decays, the typical resolution observed in the data are 20 μm and 500 μm for respectively tracks with and without SMT hits.
- **trackmedium track**
  A track is trackmedium if it fulfils the trackloose requirements and if the χ^2 per degrees of freedom is smaller than 4: $\chi^2/\text{d.o.f.} < 4$
- **tracktight track**
  A track is tracktight if it fulfils the trackmedium requirements and if it has SMT hits.

[2]Here, we follow the exact quality definition names used in the `caf_util` package and the `vjets_cafe` framework.

The p20 track quality definitions were changed in December 2009 based on studies which showed that the χ^2/d.o.f. was strongly dependent on η and luminosity (see [12]). This is understood in terms of the performance of the CFT which has its best efficiency and resolution near $|\eta| \approx 1.2$ and its poorest efficiency near $\eta = 0$, and in the increase in noise hits on tracks for higher luminosity. Changing the χ^2/d.o.f. cut from 4 to 9.5 reduced (but did not eliminate) the η and luminosity dependence of this cut. Note that the highest value of χ^2/d.o.f. stored on the TMB is 10. In addition, Model Independent Search results [13] showed that about 15% of events flagged as having high values of the p_{T} sum had central muons without any CFT hits. The tracknewmedium quality category was introduced in response and the new definitions are the following:

- **trackloose track**
  A track is trackloose if $|dca| < 0.2$ cm. If the track has SMT hit the cut is tightened to $|dca| < 0.04$ cm;

- **trackmedium track**
  A track is trackmedium if it fulfils the trackloose requirements and if the χ^2 per degrees of freedom is smaller than 4: χ^2/d.o.f. < 4;

- **tracknewmedium track**
  A track is tracknewmedium if it fulfils the trackloose requirements and if the χ^2 per degrees of freedom is smaller than 9.5: χ^2/d.o.f. < 9.5 and if there are at least 2 CFT hits on the track;

- **tracktight track**
  A track is tracktight if it fulfils the tracknewmedium requirements and if it has SMT hits.

Currently, there are data/MC SFs available for all three p17 definitions (version 1) for both p17 and p20, and the four p20 definitions (version 2) for p20 *only*.

3.4 Muon Isolation

3.4.1 Definition of Isolation Variables

The isolation cut variables are designed to separate prompt muons from electroweak processes like $Z \to \mu^+\mu^-$ and $W \to \mu\nu$, and secondary muons produced in heavy flavour quark decays $b, c \longrightarrow \mu + X$. Naturally, such muons from heavy flavour decays tend to be surrounded by additional hadronic activity from b or c fragmentation, i.e. X in the process indicated above. This fact can be used to reject secondary muons while selecting prompt ones based on tracks or calorimetric energy deposition around the muon. At the moment, three basic discrimination variables are used at DØ:

- $\Delta R \equiv \Delta R(\mu, \mathrm{jet})$,
  i.e. the distance of the muon to the central axis of the closest jet in $\eta \times \phi$ space.

- $\mathcal{I}^{\mathrm{trk}}_{\Delta R<0.5} \equiv \sum_{\{\mathrm{tracks} \in \Delta R<0.5\}} p_{\mathrm{T}}$,
  i.e. the scalar sum of transverse momenta of all tracks inside a $\Delta R(\mathrm{track}, \mu) < 0.5$ cone around the muon track with the exception of the muon track itself. For all the muons

considered in the sum $\Delta z_0(\mu, \text{track}) < 2\,\text{cm}$ is required in order to avoid additional tracks from pile-up;

- $\mathcal{I}^{\text{cal}}_{0.1<\Delta R<0.4} \equiv \sum_{\{\text{clusters}\in 0.1<\Delta R<0.4\}} E_{\text{T}}$,
  i.e. the scalar sum of transverse energies of all calorimeter clusters inside a hollow cone $0.1 < \Delta R(\text{cluster}, \mu) < 0.4$ cone around the muon. Only the energy deposits in the electromagnetic calorimeter and the first sampling of the hadronic calorimeter are considered in order to reduce the impact of noise and pile-up;

Additionally, there are two derived isolation quantities: $\mathcal{I}^{\text{trk}}_{\Delta R<0.5}/p_{\text{T}}$ and $\mathcal{I}^{\text{cal}}_{0.1<\Delta R<0.4}/p_{\text{T}}$, i.e. the basic $\mathcal{I}^{\text{trk}}_{\Delta R<0.5}$, $\mathcal{I}^{\text{cal}}_{0.1<\Delta R<0.4}$ quantities scaled by the p_{T} of the muon.
Typically, for analyses interested in high-p_{T} leptons from electroweak processes, isolation working points based on such p_{T}-scaled variables are a better choice than the non-scaled ones: due to the p_{T}-dependence they offer more rejection power for the low-p_{T} region inhibited by secondary leptons from heavy flavour decays, and on the same time provide a higher efficiency for the high-p_{T} region, where one is more likely to pick a prompt muon in the first place.

3.4.2 Definition of Isolation Working Points

The isolation working points currently in use at DØ are summarized in Table 2.

Name of working point	$\mathcal{I}^{\text{trk}}_{\Delta R<0.5}$	$\mathcal{I}^{\text{cal}}_{0.1<\Delta R<0.4}$	$\mathcal{I}^{\text{trk}}_{\Delta R<0.5}/p_{\text{T}}$	$\mathcal{I}^{\text{cal}}_{0.1<\Delta R<0.4}/p_{\text{T}}$	ΔR
TopScaledLoose	–	–	< 0.2	< 0.2	–
TopScaledMedium	–	–	< 0.15	< 0.15	–
TopScaledTight	–	–	< 0.1	< 0.1	–
TopP14	–	–	< 0.06	< 0.08	< 0.5
NPLoose	$< 4.0\,\text{GeV}$	–	–	–	–
NPTight	$< 2.5\,\text{GeV}$	$< 2.5\,\text{GeV}$	–	–	–
TrkLoose*	$< 4.0\,\text{GeV}$	$< 10.0\,\text{GeV}$	–	–	–
TrkLoose*	$< 2.5\,\text{GeV}$	$< 10.0\,\text{GeV}$	–	–	–
TrkLooseScaled*	–	–	< 0.25	< 0.4	–
TrkTightScaled*	–	–	< 0.12	< 0.4	–
hybrid	$< 3.6\,\text{GeV}$	–	–	0.12	–
deltaR	–	–	–	–	< 0.5

Table 2: The definition of isolation working points currently in use at DØ. The naming scheme as adopted in the `caf_util` and the remainder of the `vjets_cafe` framework is used. The working points available in `p20` only are marked with *. All isolation requirements other than deltaR are applicable only after the deltaR requirement is passed, and are therefore referred to as *posterior*. See Subsection 3.4.1 for the definition of ΔR, $\mathcal{I}^{\text{trk}}_{\Delta R<0.5}$, $\mathcal{I}^{\text{cal}}_{0.1<\Delta R<0.4}$.

3.5 Supported CAFE-Level DATA/MC Corrections for Muons

In the next sections of this document the efficiency measurements of muon identification criteria, tracking criteria and isolation criteria will be presented. These efficiencies are measured using

high p_{T} muons from a $Z \to \mu^+\mu^-$ sample in order to derive SFs to account for data/MC differences using the `muid_eff` and `caf_eff_utils` packages [14, 8]. The trigger object efficiencies are measured to simulate triggers using the `caf_trigger` package [9].

The efficiency corrections are valid for only the supported certified muons which are:

- of quality either loose or medium or mediumnseg3, and passing the loose cosmic veto, `IsCosmic`, or not imposing this requirement;
- matched to a high p_{T} ($p_{\mathrm{T}} > 20$ GeV) reconstructed central track of either trackloose or trackmedium or tracknewmedium* or tracktight quality;
- isolated with respect to the deltaR working point;
- isolated with respect to one one or none of the following working points which will be referred to as *posterior isolation* in the following: TopScaledLoose, TopScaledMedium, TopScaledTight, TopP14, NPLoose, NPTight, TrkLoose*, TrkLoose*, TrkLooseScaled*, TrkTightScaled*, and hybrid.

The starred (*) definitions are available only for the `p20` dataset.

It must be stressed that any departure from these definitions may require new measurements of the efficiencies. It is up to the analyser to determine to what extent the results stored in the `muid_eff` package are valid for their own purpose.

The prompt muon identification SFs are applied consecutively using several `MuonCorr` instances from the `caf_eff_utils` package. Therefore, these are factorised in four distinct categories[3]:

1. muID efficiency $\times$ cosmic veto efficiency[4] $\times$ track matching efficiency;
2. tracking efficiency;
3. isolation efficiency in deltaR;
4. isolation efficiency in one of the posterior isolation requirements.

The actual SFs are calculated on-the-fly using data and MC efficiencies stored in the `muid_eff` package.

4 Certification Samples

For the efficiency computation, the full `2MUhighpt` skim of the Summer 2009 Extended dataset has been analyzed using the packages `wzreco` and `muo_cert` to extract a clean sample of $Z \to \mu^+\mu^-$ events. The efficiency measurements rely on a "tag-and-probe" method using these $Z \to \mu^+\mu^-$ events around the Z mass peak. Figure 1 displays some basic quantities of the selected dimuon events (using the `muid_tree` tag-and-probe selection): their instantaneous luminosity, η^{CFT}, invariant mass, and muon p_{T} distributions. The data is from a run range between 222484 and 258040.

[3]The systematic uncertainties resulting from this factorisation are estimated in the respective sections for muon identification, tracking, and isolation systematics in Subsections 6.5, 7.5, and 8.5.

[4]Note, that the cosmic veto efficiency is now optional (cf. Subsection 3.2).

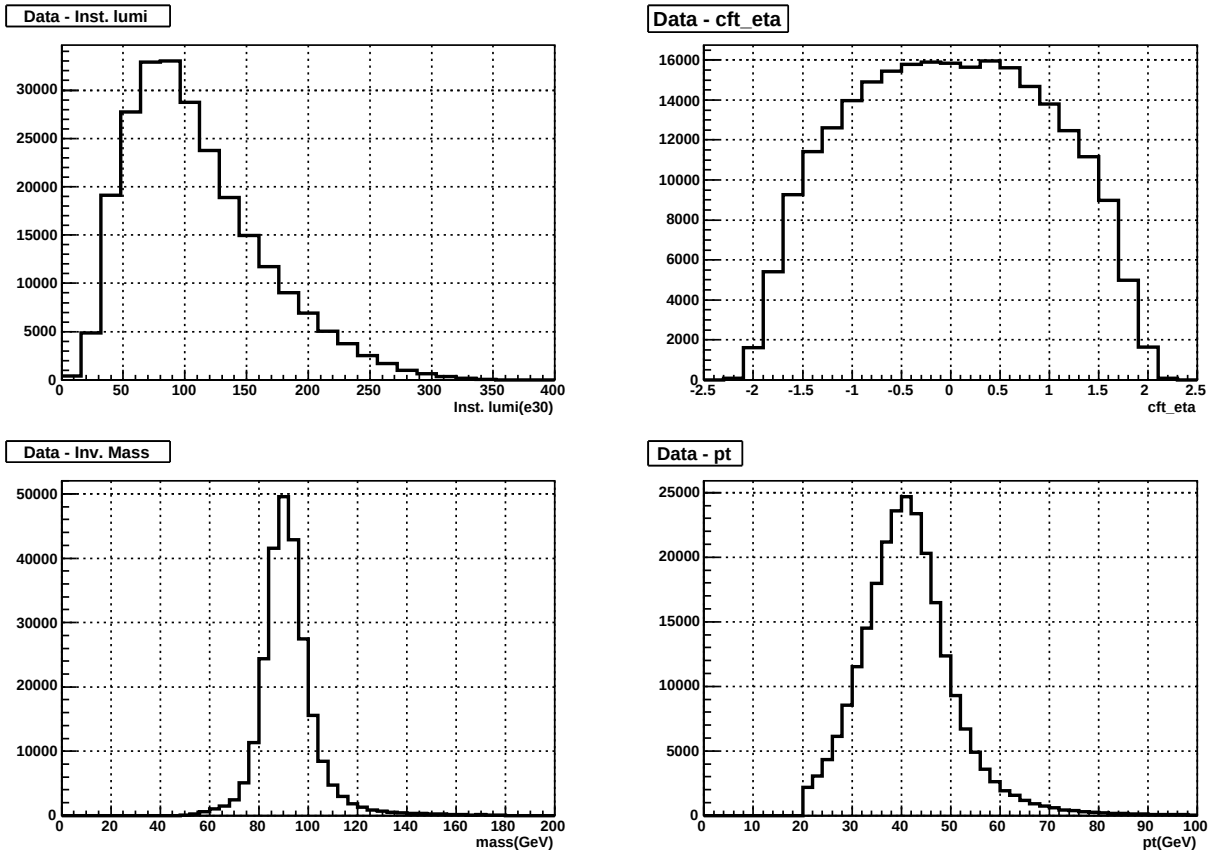

Figure 1: Instantaneous luminosity **(top left)**, muon $\eta^{\rm CFT}$ as measured at the outer boundary fo the CFT **(top right)**, dimuon mass **(bottom left)**, and muon $p_{\rm T}$ **(bottom right)** distributions in data events selected for the muon certification. See text for details.

The corresponding efficiencies for Monte Carlo were measured using a sample of simulated $Z \to \mu^+\mu^-$ events with request IDs 86872 through 86876, which were generated with Pythia.

5 Luminosity Spectrum Reweighting

The tracking and isolation efficiencies shows a pronounced dependence on the instantaneous luminosity $\mathscr{L}$(cf. Fig. 8 and 16), which is mostly due to a higher occupancy rate of the detector as well as ambiguities in the pattern recognition at high luminosities in case of tracking, and additional hadronic energy and tracks not belonging to the primary interaction in case of isolation. The luminosity dependence of the muon identification efficiency is rather small due to smaller occupancy effects. This luminosity dependence is modeled in MC by "superimposing" minimum bias data events on the simulated MC events.

The mandate of the official and central certification of prompt muon detection efficiency is to derive it in an experimental environment as similar as possible to the situation in a typical physics analysis at DØ. Thus, the pronounced luminosity dependence implies the need for luminosity reweighting. To be in-line with the vast majority of physics analyses at DØ, we

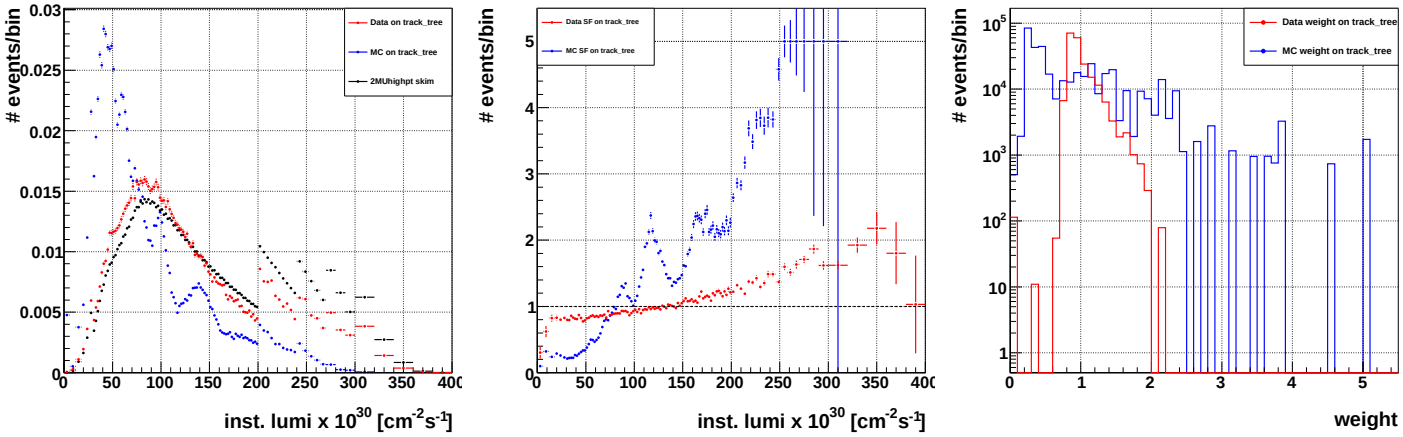

Figure 2: The normalised luminosity profile in the tag-and-probe sample for track efficiency measurements in data and MC, as well as for the `2MUhighpt` skim **(left)**, the distribution of weights versus $\mathscr{L}$ used for reweighting to the `2MUhighpt` skim **(middle)**, and the distribution of weights applied (on an event by event basis) **(right)**. Note that the discontinuities in the luminosity profile plot are due to a varying bin width.

reweight *both* our data and MC samples: the luminosity profile in data is different because we use a rather specific set of triggers in order to unbias our tag-and-probe measurement; the difference in MC comes about because only minimum bias data which was already recorded at the point when MC was produced could be used for minimum bias overlay. We reweight to the luminosity profile found in the `2MUhighpt` skim. The procedure is in-line[5] with what is done with MC at CAFe level, the only difference being that the maximum weight is restricted to 5 rather than 3. The normalised luminosity profile in the tag-and-probe sample for track efficiency measurements in data and MC, as well as for the `2MUhighpt` skim is shown in Figure 2 (left), which clearly underlines the need for reweighting, especially in the high-$\mathscr{L}$ tails. The distribution of weights applied versus luminosity and the distribution of weights given to the tag-and-probe candidate are shown in the middle/right of the same Figure. Note that the MC reaches the maximum weight limit of 5 already at $\mathscr{L} \simeq 250\,\mathrm{cm}^{-2}\mathrm{s}^{-1}$, and has no entries above about $\mathscr{L} > 320\,\mathrm{cm}^{-2}\mathrm{s}^{-1}$. However, given the luminosity distribution in Figure 1 and the distribution of weights in Figure 2 (right), the effect on the overall efficiency is negligible. We expect the situtation to improve substantially in MC with the new production round using `p20.15.xx`.

In a similar fashion, we plan to implement the beam profile reweighting in z_0 (for MC only) in future certification rounds, as is done at CAFe level. Currently, this is the dominating source of track identification systematic uncertainties (cf. Subsection 7.5).

[5]Note, that at CAFe level there is no luminosity reweighting for *data*, rather the set of triggers used by a typical physics analysis changes the luminosity profile in a marginal way from what is originally found in the skim. This is not the case here, therefore the need to reweight.

6 Muon Identification Efficiency

In this Section, the efficiencies for various muon quality criteria are presented. Their dependence in η, φ, instantaneous luminosity $\mathscr{L}$, and for different running periods are discussed. The quality criteria considered are loose, medium, and mediumnseg3. The efficiency for these qualities comprises three terms: the efficiency for finding the local muon track, the efficiency for matching with the central track, and the cosmic timing cut if this is also required.

6.1 Principle of Efficiency estimation

The muID efficiencies are computed using a tag and probe method implemented in the packages `wzreco/muo_cert` [15]. $Z \to \mu^+\mu^-$ events are selected by the `wzreco` package using the cuts on the control muon:

- loose muID quality using criteria based on the muon system only (note that due to the trigger requirement almost all of these tracks pass medium)
- A-layer scintillator $|time| < 7$ ns (B-layer time if no A-scintillator hit);
- matched to a central track of quality trackmedium;
- $p_{\mathrm{T}} > 30\,\mathrm{GeV}$;
- isolated using cuts $\mathcal{I}^{\mathrm{trk}}_{\Delta R<0.5} < 3.5$ GeV and $\mathcal{I}^{\mathrm{cal}}_{0.1<\Delta R<0.4} < 2.5$ GeV;
- fires at least one single muon trigger,

and the following cuts on the probe:

- track of trackmedium quality;
- $p_{\mathrm{T}} > 20$ GeV;
- isolated $\mathcal{I}^{\mathrm{trk}}_{\Delta R<0.5} < 3.5$ GeV $\mathcal{I}^{\mathrm{cal}}_{0.1<\Delta R<0.4} < 2.5$ GeV;
- acollinearity between tag and probe $(\pi - |\varphi_1 - \varphi_2| + |\pi - \theta_1 - \theta_2|)$ greater than 0.050 (note, this criteria did not change; earlier notes incorrectly stated this was less then 0.025);
- Oppositely charged central tracks;
- $|\Delta z_0| < 2$ cm between the tag and probe track;
- $|\Delta R| < 2$ between the tag and probe track

The probe muon is then matched (either using reconstruction central matching algorithm or the more crude $\Delta R < 0.5$) to muon identification objects to estimate the muon reconstruction efficiency.

6.2 Muon Identification Efficiency

The muon reconstruction efficiencies for loose medium, and mediumnseg3 criteria are presented as functions of the instantaneous luminosity, η, φ, and muon p_{T} Figures 3, 4 and 5. There is the well-known reduced efficiency in η in the transition from central to forward regions ($0.5 < |\eta| < 1$), and in the central bottom. The average efficiencies over the full data set are 89.2%, 80.8%, and 72.1% for the loose medium, and mediumnseg3 criteria including the cosmic time cut, and 91.2%, 82.5%, and 73.6%, respectively, without the timing cut. As most of this is due to the geometry of the muon system, the MC agrees reasonably well with efficiencies of 89.4%, 82.4% and 74.2% with timing cuts and 91.7%, 84.2% and 76.0% without timing cuts. The MC does not include the occasional loss of a detector element (like an A-layer PDT), which has its largest impact on the nseg=3 category. This can be seen in Fig. 6 where we show the efficiency for mediumnseg3 as a function of run number.

The figures show that the variation of the efficiencies as a function of instantaneous luminosity is small; possibly a few percent over the range. But as we'll see below, the muon identification efficiencies fall slightly with the quality of the central track, and this track quality worsens for high luminosity running periods. So it may be a small reduction in the matching efficiency. For this version of the SPC correction files, the efficiency numbers were determined by reweghting events such that they have the luminosity profile of the `2MUhighpt` skim rather then what passes the tag+probe selection. Determining the muon identification efficiencies with and without this weighting gave a small difference, lowering the three categories by 0.2%,

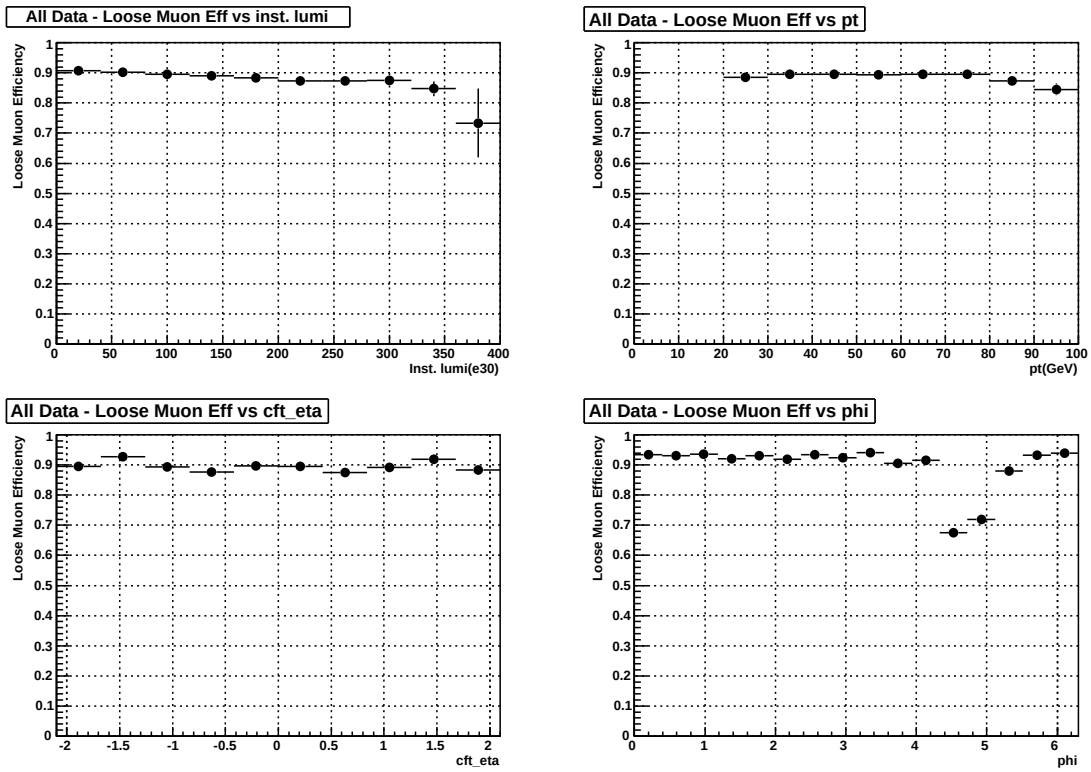

Figure 3: loose offline reconstruction efficiencies for muons passing the cosmic veto and matched to tracks versus instantaneous luminosity $\mathscr{L}$ **(top left)**, p_{T} **(top right)**, muon η **(bottom left)**, and φ **(bottom right)**.

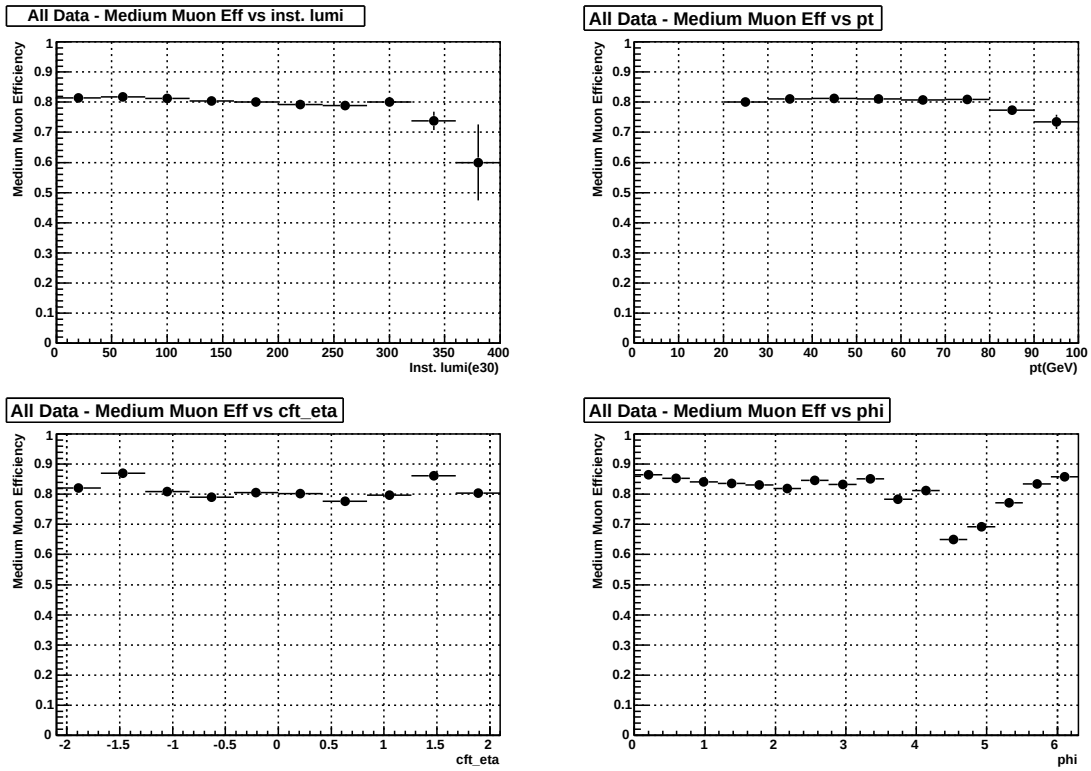

Figure 4: medium offline reconstruction efficiencies for muons passing the cosmic veto and matched to tracks versus instantaneous luminosity $\mathscr{L}$ **(top left)**, p_{T} **(top right)**, muon η **(bottom left)**, and φ **(bottom right)**.

0.2%, and 0.1%, respectively, when weighting was included.

We have seen a dependence of a few percent as a function of the p_{T} of the Z (p_{T}^{Z}). We define two samples, $p_{\mathrm{T}}^{Z} < 20$ GeV and $p_{\mathrm{T}}^{Z} > 20$ GeV, by using the p_{T}^{Z} determined from the muons or by also requiring that there not be any jet with $E_{\mathrm{T}} < 15$ GeV for the lower p_{T}^{Z} sample and requiring one or more jets for the higher p_{T}^{Z}. This jet requirement was added as we initially found that most events with higher p_{T}^{Z} were due to poorer momentum resolution on the muon tracks (one indicator was these tracks were less likely to have SMT hits). Adding the jet requirement did not seem to affect the results. Figure 7 plots the efficiency versus η for data and MC dividing the sample into $p_{\mathrm{T}}^{Z} < 20$ GeV and $p_{\mathrm{T}}^{Z} > 20$ GeV. The slightly worse efficiency is again probably due to having poorer central track quality for the higher p_{T}^{Z} events, which causes the muons to have poorer momentum resolution and therefore often higher p_{T}^{Z}. The same effect is seen in MC but with a slightly smaller decrease in efficiency; this difference will be included as a systematic uncertainty.

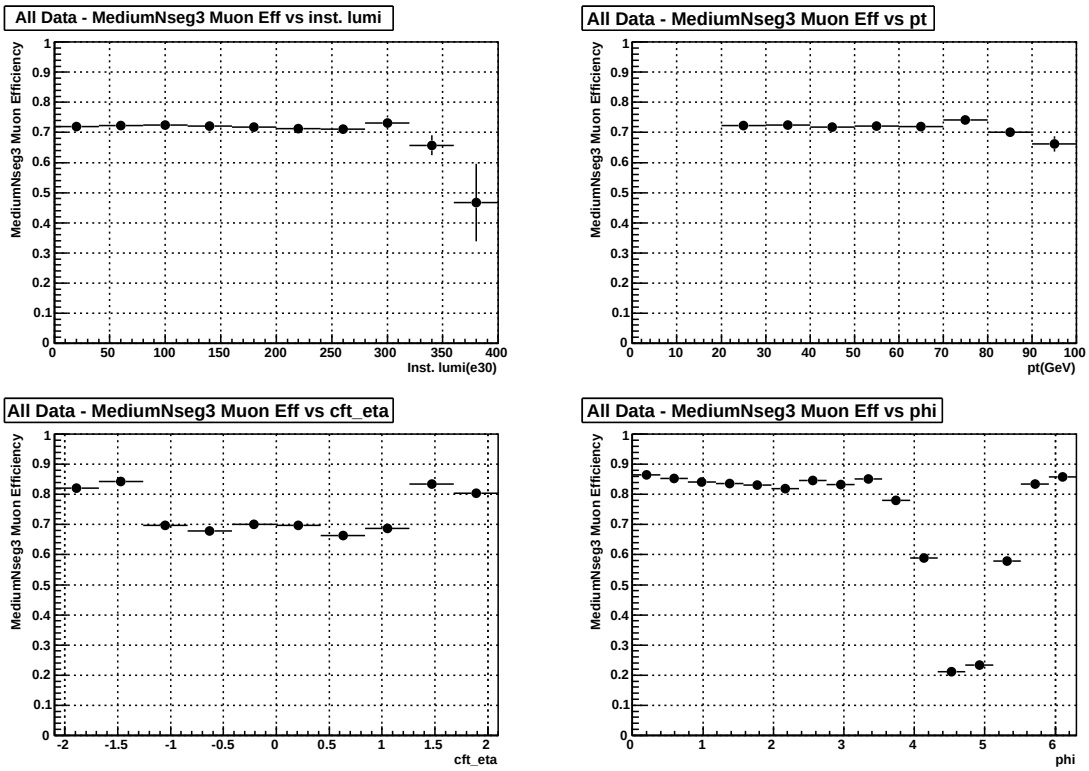

Figure 5: mediumnseg3 offline reconstruction efficiencies for muons passing the cosmic veto and matched to tracks versus instantaneous luminosity $\mathscr{L}$ **(top left)**, p_{T} **(top right)**, muon η **(bottom left)**, and φ **(bottom right)**.

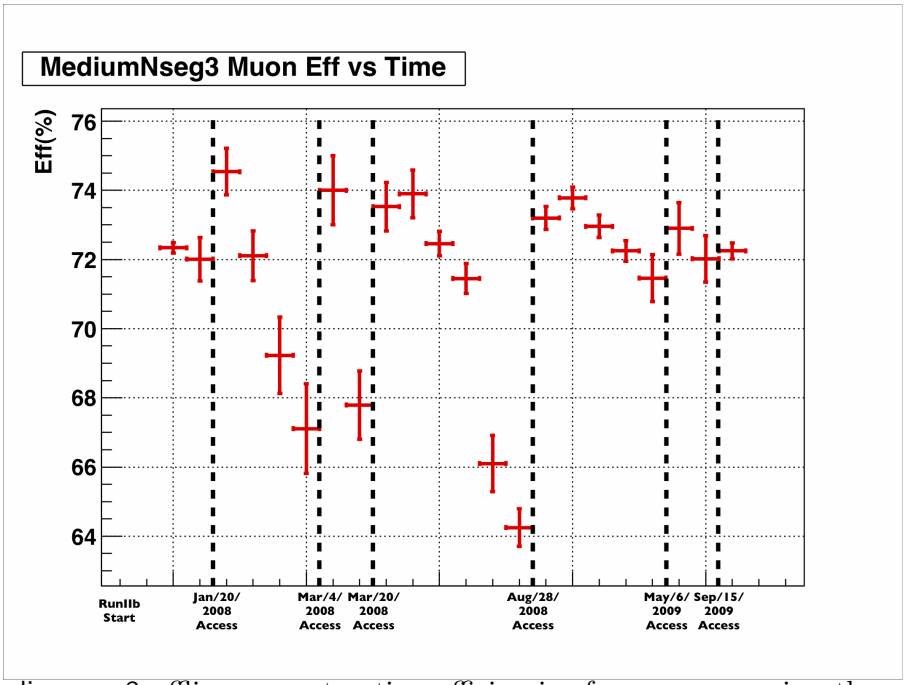

Figure 6: mediumnseg3 offline reconstruction efficiencies for muons passing the cosmic veto and matched to tracks versus run number. The figure is consistent with hardware failures and repairs. In this Figure, no reweighting in $\mathscr{L}$ is applied.

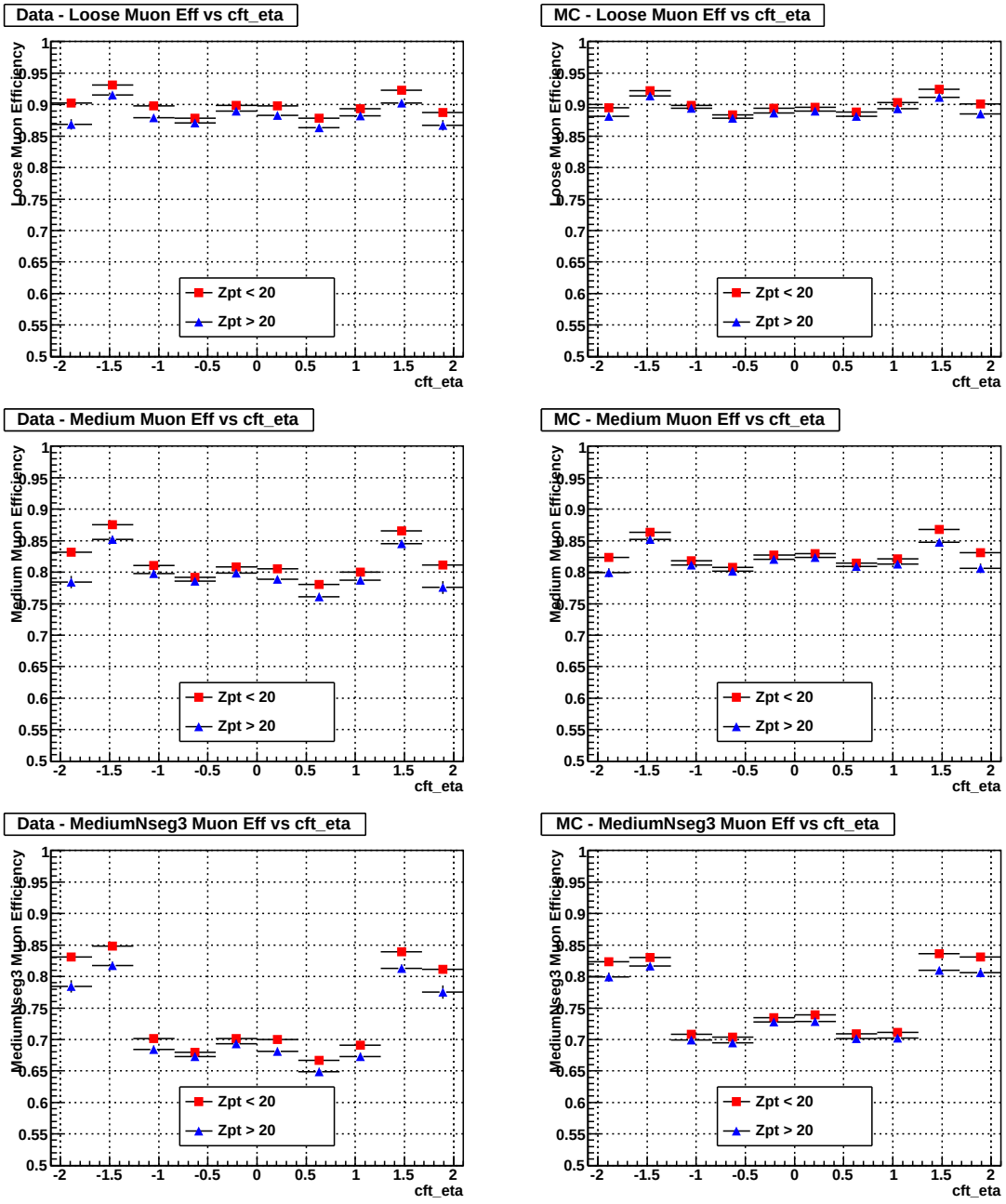

Figure 7: loose, medium, and mediumnseg3 offline reconstruction efficiencies for muons passing the cosmic veto and matched to tracks versus η for data (left) and MC (right) for $p_{\mathrm{T}}^{Z} < 20$ GeV and $p_{\mathrm{T}}^{Z} > 20$ GeV, as defined in the text.

6.3 Muon Identification Efficiency Data/MC Scale Factor Parametrisation

As seen in Fig. 7 the muID reconstruction efficiencies of simulated and real muons are slightly different. The muID times central track matching[6] times cosmic veto efficiencies are computed as a 2-dimensional function of detector η and φ by the package `muid_eff` [14] for both data and MC. The binning is:

- in φ, 25 bins of variable width in order to reflect the 8-fold detector geometry are used in the range $\varphi \in [0,\, 2\pi)$;
- in η, 38 bins are used in the range $\eta \in [-2.1,\, 2.1]$. All bins but the outer two have a width of 0.1, while the latter are 0.3 wide because of limited statistics at high $|\eta|$.

The ratio of efficiencies, data/MC, has to be applied using the `caf_eff_utils` package [8] to the simulated muons to correct for the inaccuracy of the MC.

Typically, the average correction factors are 0.998, 0.980, and 0.971 for the loose, medium, and mediumnseg3 criteria, respectively.

Note that the analyser has also to further correct for the tracking and isolation efficiency, depending on the track and isolation quality requirements.

6.4 Overall Efficiency and Data/MC Scale Factors for Muon Identification

In Table 3, the overall muon identification efficiency and muon-to-track matching efficiency, as measured on our $Z \to \mu^+\mu^-$ sample in data, is given. The efficiencies are shown with and without the cosmic veto. For comparison, the same figures are given before luminosity reweighting to the `2MUhighpt` skim spectrum. Further, the overall data/MC SFs are presented. All these overall results depend on the topology in $\eta \times \varphi$ and other variables, so are only indicative.

The muon identification efficiencies stored in the SPC files as measured in this certification round (i.e. `v05-01-02` of `muid_eff`) can be found in Ref. [18].

6.5 Systematic Uncertainty Muon Identification Efficiency Data/MC Scale Factors

Several sources of uncertainty may affect efficiency measurements and data/MC correction factors. A number of these sources including tag-and-probe biases, backgrounds, and statistics, were investigated in the `p17` note [1] and will not be discussed further here. They are included in the table below straight from this note except for the cut variation. This was found in the 2008 `p20` note [2] to be somewhat larger when the central tracking category was varied. We have also found a variation with the p_{T} of the Z which is probably also related to track quality and therefore the matching efficiency. We have added a term of 0.3 % to account for the data vs MC differences.

[6] Track matching efficiency is the efficiency that a muon reconstructed in the muon system and the corresponding reconstructed central track are matched together. Typically, it is of the order of 99%.

Statistical figure	loose	medium	mediumnseg3
Efficiency in data	$89.2 \pm 0.1\,\%$	$80.8 \pm 0.1\,\%$	$72.1 \pm 0.1\,\%$
Efficiency in data (w/o $\mathscr{L}$ rew.)	$89.4 \pm 0.1\,\%$	$81.0 \pm 0.1\,\%$	$72.2 \pm 0.1\,\%$
data/MC SF	0.998 ± 0.001	0.980 ± 0.001	0.971 ± 0.001

Statistical figure	looseNCV	mediumNCV	mediumnseg3NCV
Efficiency in data	$91.2 \pm 0.1\,\%$	$82.5 \pm 0.1\,\%$	$73.2 \pm 0.1\,\%$
Efficiency in data (w/o $\mathscr{L}$ rew.)	$81.3 \pm 0.1\,\%$	$82.6 \pm 0.1\,\%$	$73.6 \pm 0.1\,\%$
data/MC SF	0.995 ± 0.001	0.979 ± 0.001	0.969 ± 0.001

Table 3: Figures for overall muon identification and muon-to-track matching efficiency, as well as data/MC SFs, as measured on our $Z \to \mu^+\mu^-$ sample in data. The efficiencies are shown with and without the cosmic veto (in the latter case, "NCV" is appended to the muon quality name). All uncertainties given in this Table are statistical only. For details see text.

In 2007 and 2008 a series of studies were done on a sample of about 2000 Zs. For about 50 events where no loose muon was found, the events were dumped and searched for evidence of hits in the muon system at the (η, φ) of the probe's central track. In most cases there were no hits as the track was in the region of the detector which lacked muon coverage. This is also seen in the (η, φ) plots of inefficient tracks. But for about 1 % of these events, there were hits. By varying the code used to form segments and then combine segments into tracks, these events could be recovered. Essentially the local muon segment's position and angle values had been mis-determined causing the local track not to match with the central track. But while some events were recovered, other events were then lost. Tuning the parameters for the sub-sample at hand gave an increase in efficiency. It also changed at the 2 % level what category (nseg=2 versus nseg=3, loose versus medium) the muon track had. However when this was used on an untuned sample, no improvement was seen and the requirements in `d0reco` were not changed. While we then measure the efficiency this indicated a small systematic error on the pattern recognition for loose muons and a somewhat larger systematic for medium muons, which for the 2008 p20 note was estimated to be $< 0.4\,\%$. It is also partially accounts for the somewhat lower efficiency seen in the data compared to MC for the medium category, which is dominated by nseg=3 events.

The systematic uncertainty for luminosity and time variations is taken to be 0. As seen in Figures 3-5, the muon identification categories have very little variation with instantaneous luminosity, and the efficiencies are weighted for the `2MUhighpt` luminosity profile. The efficiencies will vary in time mostly due to variations in the detector hardware. For example, a missing A-layer PDT will cause a reduction in the nseg=3 category (and also in the trigger efficiency). As we determine the efficiency for the entire data sample, this is measured but a systematic error of about 2 % should be expected between different running periods. Also, the values in the table are for muon $p_{\mathrm{T}} > 20\,\mathrm{GeV}$. If this is extrapolated to lower p_{T} then a systematic uncertainty needs to be applied[7], which we estimate to be 2 % for all categories.

The limited size of our Z-sample in data and MC results in a statistical uncertainty on the data/MC SF. For data, it amounts to 0.06 %, 0.08 %, 0.09 % for loose, medium, mediumnseg3

[7]Note, that this uncertainty needs to be applied *only* to the fraction of the spectrum below $p_{\mathrm{T}} < 20\,\mathrm{GeV}$.

Source of systematic	loose	medium	mediumnseg3
tag-and-probe bias	0.2 %	0.2 %	0.2 %
background and cut variations	0.8 %	1.1 %	1.1 %
Z boson p_{T} variation	0.3 %	0.3 %	0.3 %
luminosity and time	–	–	–
pattern recognition	0.0 %	0.4 %	0.4 %
statistical (V + jets)	0.1 %	0.1 %	0.1 %
statistical (other processes)	0.2 %	0.2 %	0.2 %
Total w/o statistical	0.9 %	1.2 %	1.2 %
Total (other processes)	**0.9 %**	**1.1 %**	**1.2 %**
time average, up to	*2.0 %*	*2.0 %*	*2.0 %*
$p_{\mathrm{T}} < 20\,\mathrm{GeV}$, *fractional*	*2.0 %*	*2.0 %*	*2.0 %*

Table 4: Summary of systematic uncertainties on the muon identification data/MC scale factors. For a typical physics analysis all systematic uncertainties including the one from limited Z-sample statistics are applicable. The uncertainty due to limited statistics is uniformly taken as 0.1 % for all V + jets processes, whereas 0.2 % is conservatively assumed for all other processes, which may sample the bins (and thus statistical uncertainties) with a different frequency. The uncertainty due to a shorter time period of the Summer 2009 Extended dataset and due to $p_{\mathrm{T}} < 20\,\mathrm{GeV}$ may be applicable for some analyses (both in italic). For details see text.

requirements, respectively. The corresponding values for MC are well below data due to a larger sample size. Across all track quality requirements, we uniformely quote an uncertainty of 0.1% on the data/MC SFs due to limited statistics.

Note, that the above SF uncerainty is valid ony for V+jets processes, whereas an uncertainty of 0.2 % should be conservatively assumed for all other processes, which may sample the SF bins (and thus statistical uncertainties) with a different frequency.

As of `p21-br-16` of the `caf_eff_util` package it is possible to access the statistical uncertainties in CAF on an event-by-event basis via the `stat` processor. Some analyses may choose to use this approach rather than a flat uncertainty we centrally provide.

6.5.1 Systematics Summary

The uncertainties on data/MC muon identification efficiency scale factors due to possible systematic biases discussed above are summarized in Table 4.

7 Track Reconstruction Efficiency

In this part, the efficiencies of tracking for various track quality criteria are presented, and their dependence on luminosity is discussed.

7.1 Principle of Efficiency Estimation

The tracking efficiencies are computed using a tag and probe method implemented in the packages `wzreco/muo_cert` [15]. The selection is identical to the previous `p20` and `p17` results except that a calorimeter isolation cut is now imposed on the probe muon. It is seen that this new requirement reduces the background by about 50% and thereby the measured efficiencies increased by about 1%.

$Z \to \mu^+\mu^-$ events are selected by the `wzreco` package using the following cuts on the control muon:

- loose muonid quality (using criteria based on the muon system only);
- matched to a central track;
- $p_{\mathrm{T}} > 30$ GeV;
- $|dca| < 200$ μm (where dca, also referred to as d_0, is the transverse impact parameter with respect to the beam position);
- isolation using cuts $\mathcal{I}^{\mathrm{trk}}_{\Delta R<0.5} < 3.5$ GeV and $\mathcal{I}^{\mathrm{cal}}_{0.1<\Delta R<0.4} < 2.5$ GeV,

and the following cuts on the probe muon:

- loose muon identification quality (using criteria based on the muon system only);
- $p_{\mathrm{T}}^{\mathrm{loc}} > 15$ GeV, where $p_{\mathrm{T}}^{\mathrm{loc}}$ is the muon p_{T} measured in the muon system *only*;
- $\Delta R > 2$ between the tag and probe muons;
- $\Delta t < 6$ ns, where Δt is the time difference between scintillator hits in either A- or B-layer of the tag and probe muons;
- calorimeter isolation $\mathcal{I}^{\mathrm{cal}}_{0.1<\Delta R<0.4} < 2.5$ GeV

To remove any possible trigger bias, the events are required to fire a dimuon trigger with no track requirement.

7.2 Track Reconstruction Efficiency

The track reconstruction efficiencies for the four track qualities are presented as a function of the instantaneous luminosity in Figure 8 for both data and MC. On average, the tracking efficiencies are 91.7%, 87.1%, 90.8%, and 83.9% for the trackloose, trackmedium, tracknewmedium and tracktight tracking criteria, respectively. These values include reweighting in $\mathscr{L}$ to the `2MUhighpt` luminosity profile (without re-weighting, the values would be 92.0%, 87.5%, 91.0%,

and 83.6%). About 4-5% of the probe muons do not have any associated tracks, and an additional 4-5% fail the $|dca|$ cut. The change in definition of the $|dca|$ cut (from 0.02 cm to 0.04 cm if there are SMT hits) is small, and the resultant efficiency change is less than 0.5% and mostly affected by muons with $p_{\mathrm{T}} < 30$ GeV. All of these efficiencies fall with instantaneous luminosity as shown in the figure. However, with the change in definition, the tracknewmedium tracks undergo only about half the luminosity dependence that is seen with the trackmedium tracks.

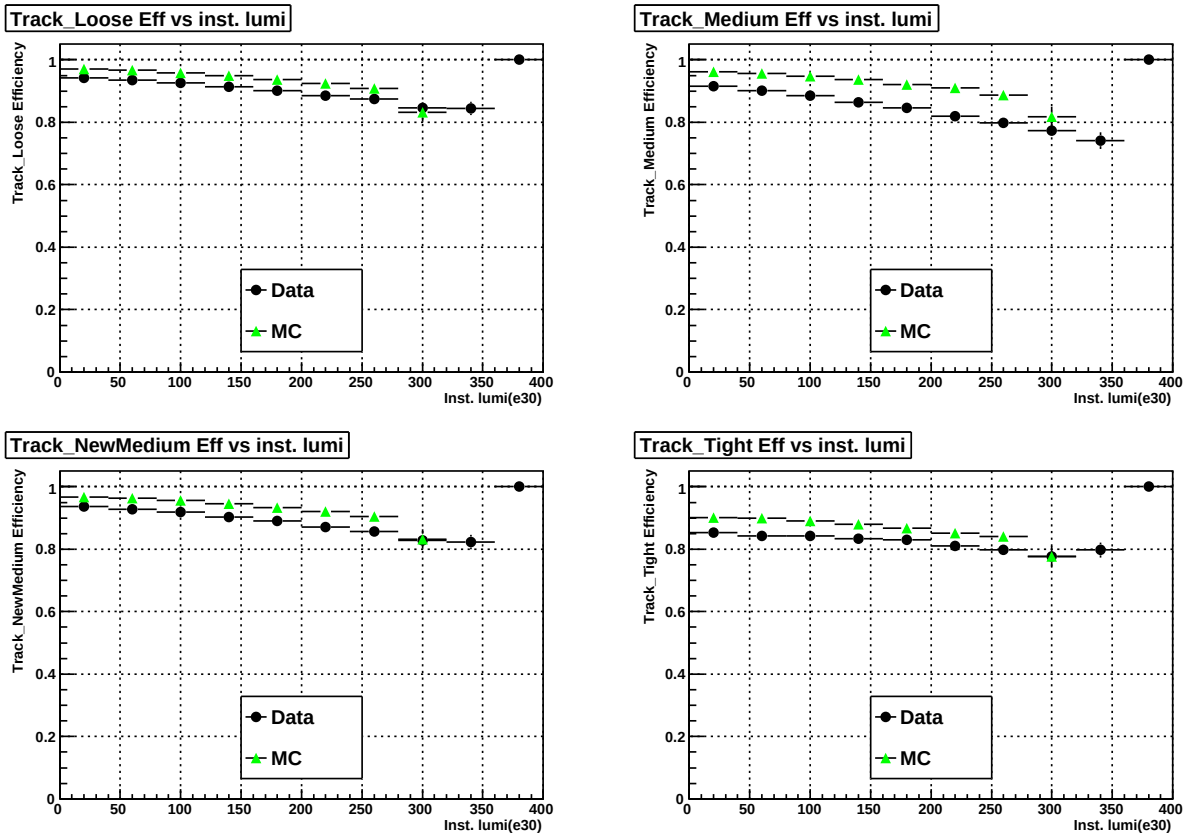

Figure 8: Efficiencies versus instantaneous luminosity for trackloose **(top left)**, trackmedium **(top right)**, tracknewmedium **(lower left)**, and tracktight **(lower right)**.

Similar to the discussion in the muon identification section, the tracking efficiencies are examined as a function of the transverse momentum of the Z boson (p_{T}^{Z}). As the tracking efficiency is strongly correlated with the track quality, which in turn is strongly correlated with the momentum resolution, we aren't able to completely separate effects. We select events where the p_{T}^{Z} is determined by requiring that both central tracks are found. Most of the inefficiency is seen to occur at the *dca* cut level. Figure 9 presents the trackloose tracking efficiencies for two samples ($p_{\mathrm{T}}^{Z} < 20$ GeV and $p_{\mathrm{T}}^{Z} > 20$ GeV) with or without jets. For $p_{\mathrm{T}}^{Z} < 20$ GeV, the efficiency is about 99% regardless of the jet requirement, which reflects that most of the tracks satisfy the loose quality criterion. However, for $p_{\mathrm{T}}^{Z} > 20$ GeV, the efficiency is sensitive to the jet requirement, indicating that the p_{T}^{Z} has a correlation with the number of jets in the event. The efficiency is about 72% with no jets, 86% with jets, and 88% with jets and the $aco > 1.5$

requirement. In this last category are events where the Z bosons are most likely to have a true p_{T} greater than 20 GeV. The MC also has some inefficiency, about 5%, for $p_{\mathrm{T}}^{Z} > 20$ GeV events. But as also seen in the Figure, the MC and data have different η dependence. Figure 10 shows the efficiencies for the two p_{T}^{Z} categories for the other three tracking quality criteria.

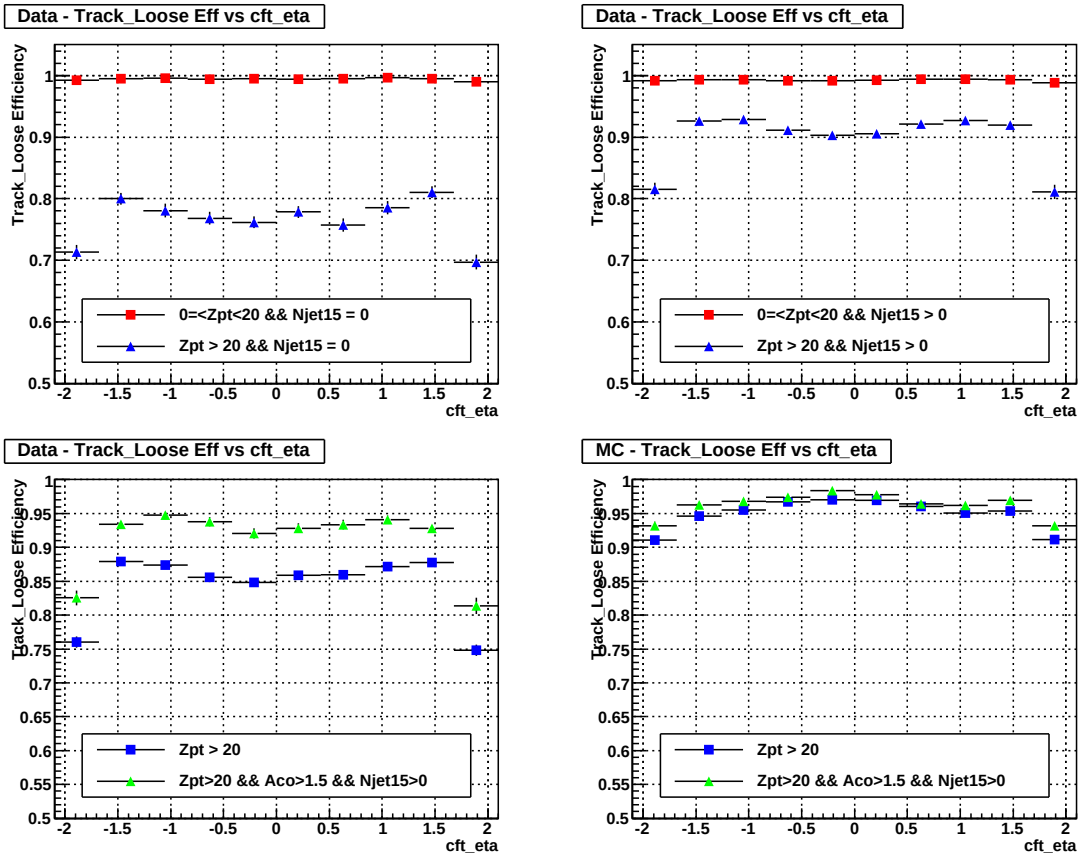

Figure 9: trackloose tracking efficiencies for $p_{\mathrm{T}}^{Z} < 20$ GeV and $p_{\mathrm{T}}^{Z} > 20$ GeV samples in data with no jets **(top left)** and at least one jet **(top right)**. An effect of the jet plus $aco > 1.5$ requirement on efficiency for the $p_{\mathrm{T}}^{Z} > 20$ GeV sample is also shown in data **(lower left)** and MC **(lower right)**.

7.3 Track Reconstruction Efficiency Data/MC Scale Factor Parameterization

As already mentioned, the tracking efficiency data/MC SFs are now applied in two steps:

- firstly, the "geometrical" track reconstruction efficiency data/MC SF parametrized in $\eta_{\mathrm{CFT}} \times z_0$ is applied;
- secondly, the luminosity dependence is corrected by a SF parametrized in $|\eta_{\mathrm{CFT}}| \times \mathscr{L}$. A parametrization in $\mathscr{L}$ alone would have been insufficient, as the impact of detector occupancy due to higher luminosity varies with η and tends to be more adverse in the central region, as shown in Figure 11.

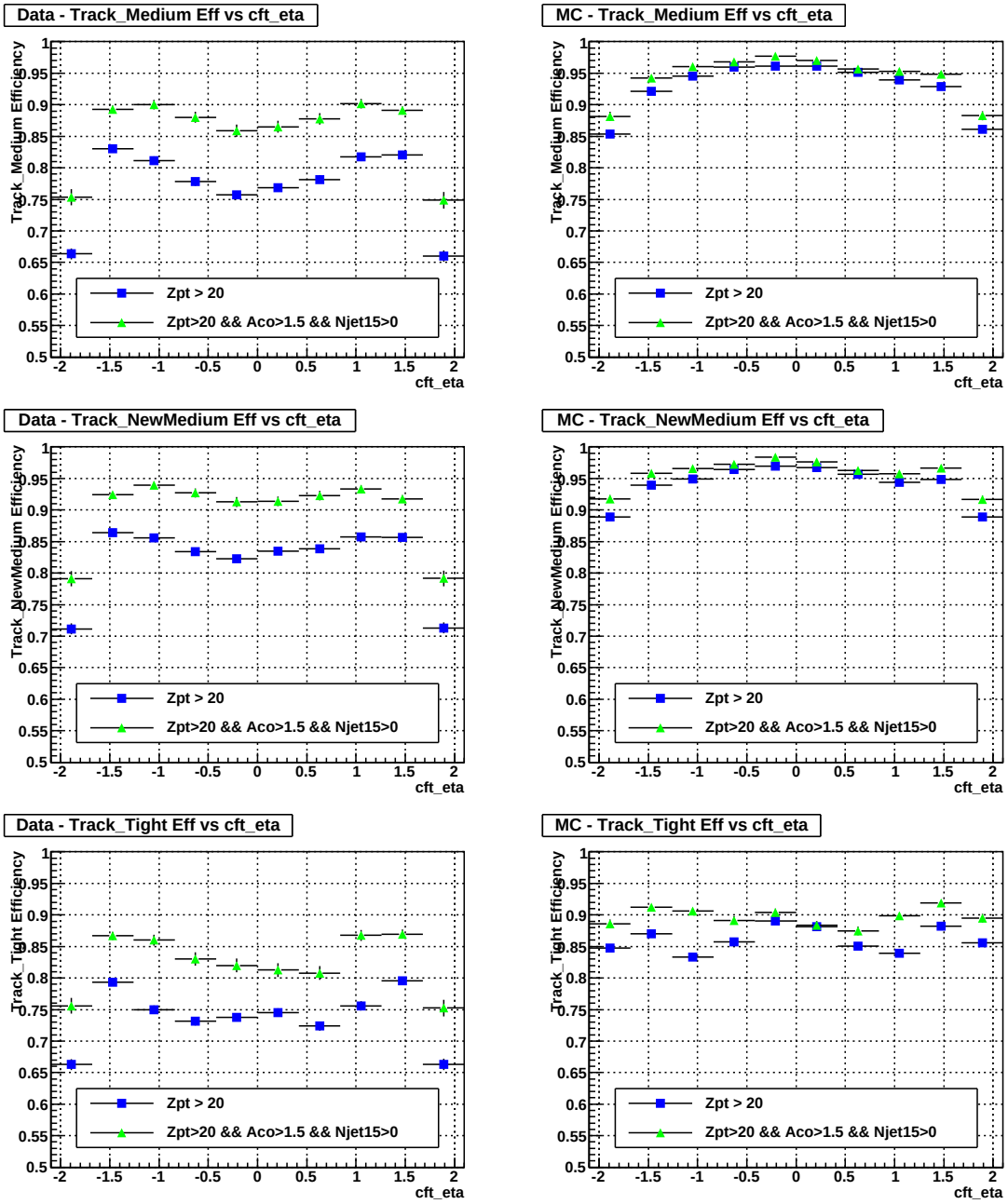

Figure 10: trackmedium, tracknewmedium, and tracktight tracking efficiencies for $p_{\mathrm{T}}^{Z} > 20$ GeV and for $p_{\mathrm{T}}^{Z} > 20$ GeV with at least one jet and $aco > 1.5$ in data **(left)**, and MC **(right)**.

Thus, the data/MC SFs are factorised, i.e. we apply the correction parametrized in $\eta_{\mathrm{CFT}} \times z_0 \oplus |\eta_{\mathrm{CFT}}| \times \mathscr{L}$. We perform this factorization such that the overall efficiency is preserved: when deriving the SFs for the luminosity dependence, we use normalized efficiencies.
The "geometrical" tracking efficiency uses the following binning:

- in η_{CFT}, we use 36 bins:
  $\{0, 0.1, 0.2, 0.3, 0.4, 0.5, 0.6, 0.7, 0.8, 0.9, 1, 1.1, 1.2, 1.3, 1.4, 1.5, 1.6, 1.8, 2.5\}$

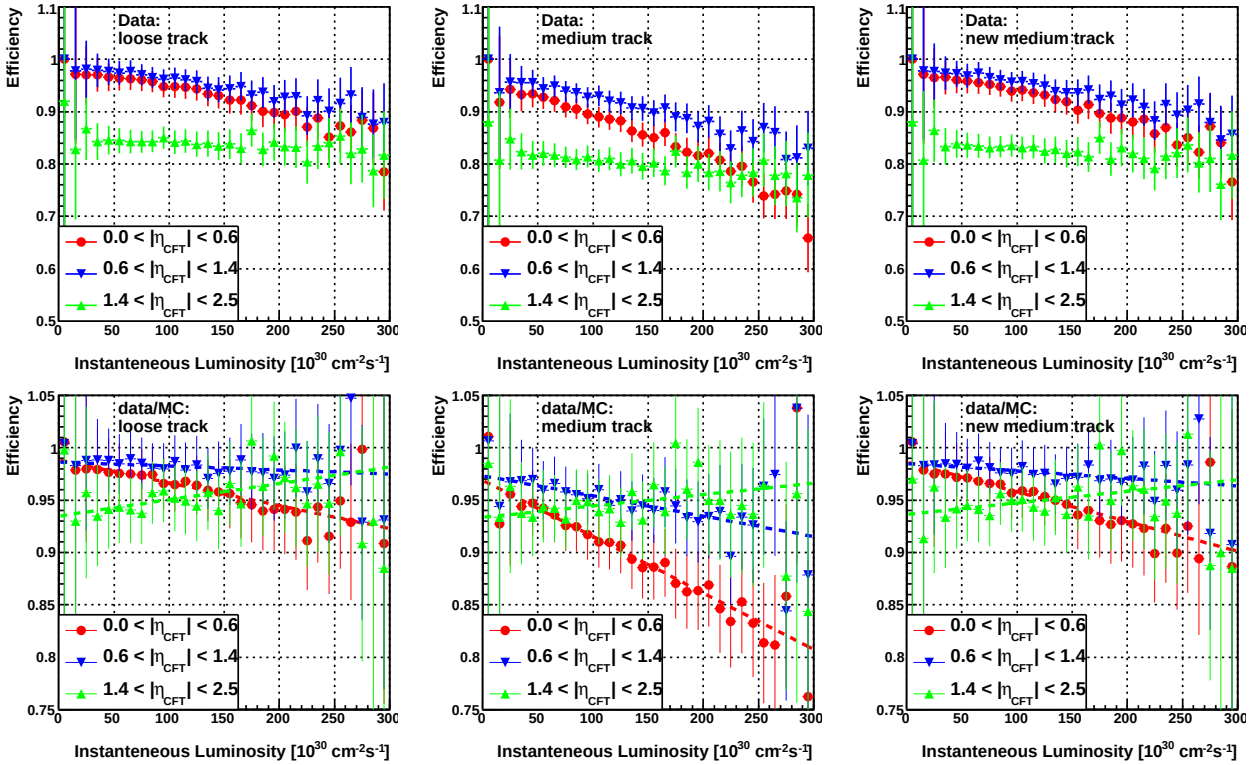

Figure 11: Tracking efficiency for muons in data **(top row)** for the working points trackloose **(left column)**, trackmedium **(middle column)**, and tracknewmedium **(right column)**. The data/MC SFs are shown in respective order in the **bottom row**, together with a linear fit to each of the distributions.

and the same for the $\eta_{\mathrm{CFT}} < 0$ side;

- in z_0, we use 8 bins: $\{-60,\ -40,\ -15,\ -5,\ 0,\ 5,\ 15,\ 40,\ 60\,\mathrm{cm}\}$.

The luminosity tracking efficiency is parametrized with the binning:

- in $\mathscr{L}$, we use 5 bins: $\{0,\ 65,\ 100,\ 145,\ 190,\ 300\,\mathrm{cm}^{-2}\mathrm{s}^{-1}\}$;
- in $|\eta_{\mathrm{CFT}}|$, we use 4 bins: $\{0,\ 0.5,\ 1,\ 1.5,\ 2,\ 2.5\}$

Typically, the average correction factors are respectively 0.964, 0.927, 0.956, and 0.947 for respectively the trackloose, trackmedium, tracknewmedium, and tracktight criteria.

7.4 Overall Efficiency and Data/MC Scale Factors for Tracking

In Table 5, the overall tracking efficiency, as measured on our $Z \to \mu^+\mu^-$ sample, is given. For comparison, the same figure is given before luminosity re-weighting to the `2MUhighpt` skim spectrum. Further, the overall data/MC SFs are presented. All these overall results depend on the topology in $\eta \times \varphi \times z_0$ and other variables, and thus are only indicative.

The muon track reconstruction efficiencies stored in the SPC files as measured in this certification round (i.e. `v05-01-02` of `muid_eff`) can be found at [18].

Statistical figure	trackloose	trackmedium	tracknewmedium	tracktight
Efficiency in data	$91.7 \pm 0.1\,\%$	$87.1 \pm 0.1\,\%$	$90.8 \pm 0.1\,\%$	$83.9 \pm 0.1\,\%$
Efficiency in data (w/o $\mathscr{L}$ rew.)	$92.0 \pm 0.1\,\%$	$87.5 \pm 0.1\,\%$	$91.0 \pm 0.1\,\%$	$83.6 \pm 0.1\,\%$
data/MC SF	0.964 ± 0.001	0.927 ± 0.001	0.956 ± 0.001	0.947 ± 0.001

Table 5: Figures for overall tracking efficiency and data/MC SFs, as measured on our $Z \to \mu^+\mu^-$ sample in data. All uncertainties given in this Table are statistical only. For details see text.

7.5 Systematic Uncertainty Tracking Efficiency Data/MC Scale Factors

Several sources of uncertainty may affect efficiency measurements, and the resulting data/MC scale factors. In the following, we try to assess them quantitatively for a typical physics analysis. For some specific reason, the reader may find that these numbers can not be applied in a straight forward way to their analysis.

7.5.1 Tag-and-Probe Biases

There are two inherent sources for potential biases in the tag-and-probe method: firstly, biases of the method per se, and secondly, biases due to the differences in the sample selection for data and MC, i.e. due to trigger effects. We address them separately:

- Existence of a possible per se bias in the method has been quantitatively assessed in [17] (`p14-pass1`) by looking at the difference between the tag and probe measurements and the genuine efficiency in MC events. The bias is found to be 0.2 %. The study has not been repeated within `p20`, but the results are thought to remain valid.
- Similarly to the muon identification case, a possible bias can be expected due to the trigger condition requirement, which is present in data, but not in MC.

Based on the results above, we quote an overall systematic uncertainty of data/MC SFs due to possible biases in the tag-and-probe method of 0.3 %.

7.5.2 Background Contamination

The presence of backgrounds in data may bias the efficiency towards lower values. This effect is not present in the pure-signal $Z \to \mu^+\mu^-$ MC and needs to be accounted for. Possible background contributions are expected for example from QCD heavy flavour production, where both the tag and the probe are muons from heavy flavour decays passing isolation criteria, or $W \to \mu\nu$, where the tag is a high p_{T} muon, whereas the probe muon can come from associate (heavy flavour) jet production. To reduce the contribution of this type of backgrounds, an explicit cut on the calorimetric isolation of the probe muon $\mathcal{I}^{\mathrm{cal}}_{0.1<\Delta R<0.4} < 2.5\,\mathrm{GeV}$ has been included in this round of certification. This has increased the measured efficiency in data by 1.5 %, 1.8 %, 1.6 %, and 1.7 % for trackloose, trackmedium, tracknewmedium, and tracktight, respectively, whereas MC was affected only by about 0.7 %. We estimate that the little remaining background contamination could account for a systematic bias about half as large as the change

in the data/MC SF resulting from the introduction of the $\mathcal{I}^{\mathrm{cal}}_{0.1<\Delta R<0.4} < 2.5\,\mathrm{GeV}$ requirement on the probe, i.e. 0.5 % for all track quality requirements.

In the p17 certification round [1], the amount of backgrounds has been estimated by varying cuts on $\Delta\varphi(\mathrm{tag},\mathrm{probe})$, d_0 (dca) of the control muon, and by imposing $N_{\mathrm{jet}} = 0$. These requirements are supposed to change the signal/background composition of the selected data sample. A systematic uncertainty due to background contamination of about 0.4 % for track definitions similar to the ones used today has been found.

Based on the findings presented above, we quote a 0.5 % uncertainty for all track quality requirements.

7.5.3 Correlation with Muon Quality

The correlation of the measured tracking efficiencies with the muon quality has been investigated in data, and found to be 0.02 %, 0.02 %, 0.02 %, and 0.01 %, for trackloose, trackmedium, tracknewmedium, and tracktight, respectively. Due to the negligible effect magnitude of notably less than 0.1 %, we disregard this systematic uncertainty.

7.5.4 Instantaneous Luminosity Dependence

As seen in Figure 11 on page 26, the tracking efficiency shows a notable dependence on the instantaneous luminosity $\mathscr{L}$, which is mostly due to a higher occupancy rate of the detector and ambiguities in the pattern recognition at high luminosities. Naturally, this dependence is more pronounced in the forward region. These variations in tracking efficiencies are not completely reproduced in the current MC. Moreover, the luminosity spectrum in data is biased by the specific choice of (mostly prescaled) triggers. Due to these factors, the tracking efficiency SFs are now being explicitly parametrised in luminosity. Owing to this, there is no systematic uncertainty due to the luminosity spectrum.

7.5.5 Jet Multiplicity Dependence

The tracking efficiency is dependent on the amount of (hadronic) activity in an event for similar reasons as laid out in Subsection 7.5.4. This is strongly correlated with the p^Z_{T} of the dimuon system and we assume that the uncertainty given in this Subsection covers both sources. The MC simulations currently in use at DØ model this dependency to some degree, however some disagreement between data and MC remains. Figure 10 showed that MC had about half the roughly 10 % efficiency reduction seen in data for higher p^Z_{T}. We also investigated the variation of the data/MC SFs in the 0, 1, 2, and 3+ jet multiplicity bins compared to the average SF value for each of the four track quality definitions, as shown in Figure 12. Based on the magnitude of the SF variation and considering the statistical uncertainty in the high jet multiplicity bins, we quote a systematic uncertainty between $o(0.1\,\%)$ for the 0, 1 jet bins and $o(1\,\%)$ for the 3 jet bin. The exact value for each track quality working point is given in the summary of systematic uncertainties in Table 6.

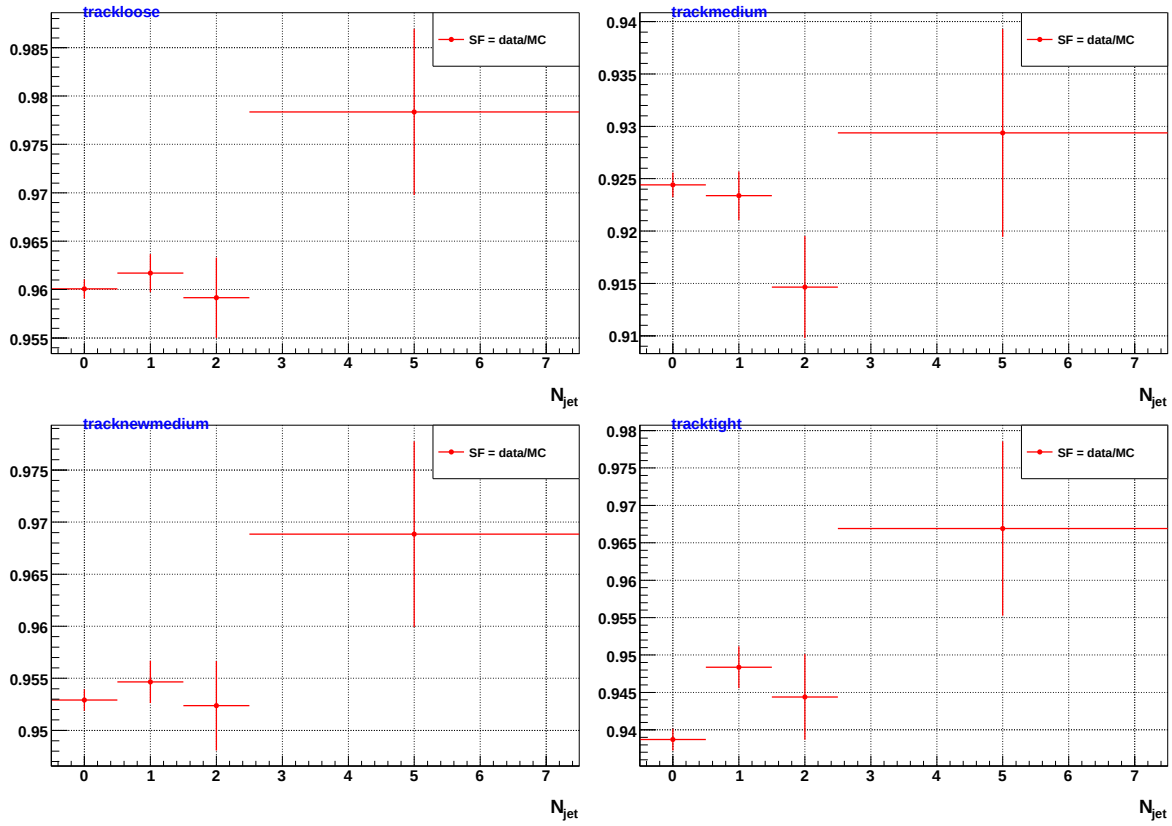

Figure 12: Data/MC SFs versus jet multiplicity N_{jet} passing trackloose **(top left)**, trackmedium **(top right)**, tracknewmedium **(lower left)**, tracktight **(lower right)** criteria. See text for figure discussion in the context of N_{jet} systematics.

7.5.6 Simulation of the Vertex Position in z

The tracking efficiency is highly dependent upon the z of the primary vertex. The shape of the beam is used to reweight the z_{MC} distribution of $Z \to \mu^+\mu^-$ MC muons passing the four tracking criteria. Weight factors from 0.8 to 1.4 are seen for $|z| < 60$ cm. The differences in the tracking efficiencies between no weighting and weighting to the shape as seen in data are seen to vary by 0.7-0.8% and we assign this as a systematic uncertainty.

7.5.7 Limited Z-sample Statistics

The limited size of our Z-sample in data and MC results in a statistical uncertainty on the data/MC SF. For data, it amounts to 0.06 %, 0.08 %, 0.07 %, 0.09 % for trackloose, trackmedium, tracknewmedium, and tracktight requirements, respectively. The corresponding values for MC are well below data due to a larger sample size. Across all track quality requirements, we uniformly quote an uncertainty of 0.1% on the data/MC SFs due to limited statistics.

Note, that the above SF uncertainty is valid only for V + jets processes, whereas an uncertainty of 0.2 % should be conservatively assumed for all other processes, which may sample the SF bins (and thus statistical uncertainties) with a different frequency.

As of `p21-br-16` of the `caf_eff_util` package it is possible to access the statistical uncertainties in CAFe on an event-by-event basis via the `stat` processor. Some analyses may choose to use this approach rather than a flat uncertainty we centrally provide.

7.5.8 Time Dependence

The efficiencies can vary with time, especially for tracktight where a SMT is required. While the efficiencies are determined for the entire sample, we have investigated the time dependence by changing the relative weight of the IIb-1 to IIb-2 samples by 20%, and saw a variation of 0.03%, essentially negligible. However we have included a systematic if one uses a different sample.

7.5.9 φ isotropy

By computing the efficiency in a (z,η) map we average out possible φ variations. Such variations are expected to happen for example because of different length of the optical fibre as a function of φ for the CFT detector. The dead channel pattern of the SMT detector is also far from being uniform in φ. This is seen in Figs. 13 and 14. Some of the variation in efficiency is seen in MC (and we anticipate that the MC distribution will change when a new version is available) but there are still differences in the data/MC efficiency versus φ on the order of 2-3%, with the σ's seen in the figures of 1.8%, 2.3%, 1.9%, and 3.3% for trackloose, trackmedium, tracknewmedium, and tracktight respectively. The efficiencies in the SPC files are obtained for the φ distribution of the dimuon tag+probe sample and there is therefore no systematic error if the φ distribution in a physics analysis is identical. If the φ distribution is different and no reweighting is performed, then there will be an additional systematic which will be a fraction (0.1-0.3) of the σ's given above, and we use $0.3 \times \sigma$ for the values in the summary table.

7.5.10 Systematics Summary

The uncertainties on data/MC tracking efficiency scale factors due to possible systematic biases discussed above are summarized in Table 6.

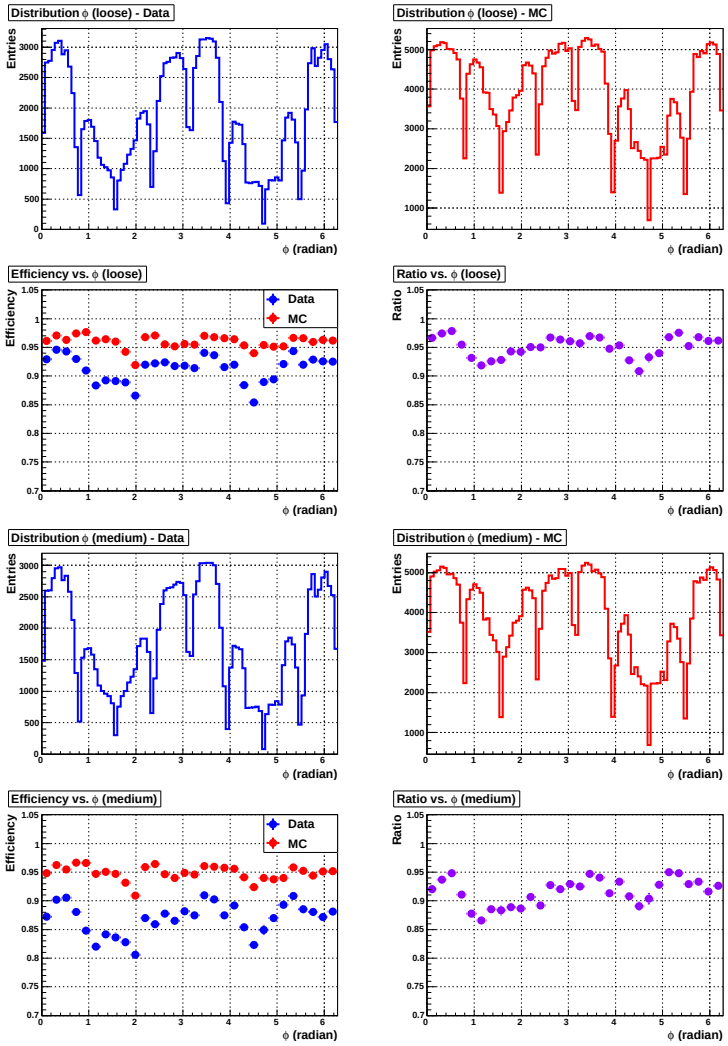

Figure 13: The distributions in φ for tracks passing trackloose for data **(top left)** and MC **(top right)**, their efficiencies versus φ **(2nd left)**, and the data/MC ratio versus φ **(2nd right)**. The same four plots are also shown passing trackmedium.

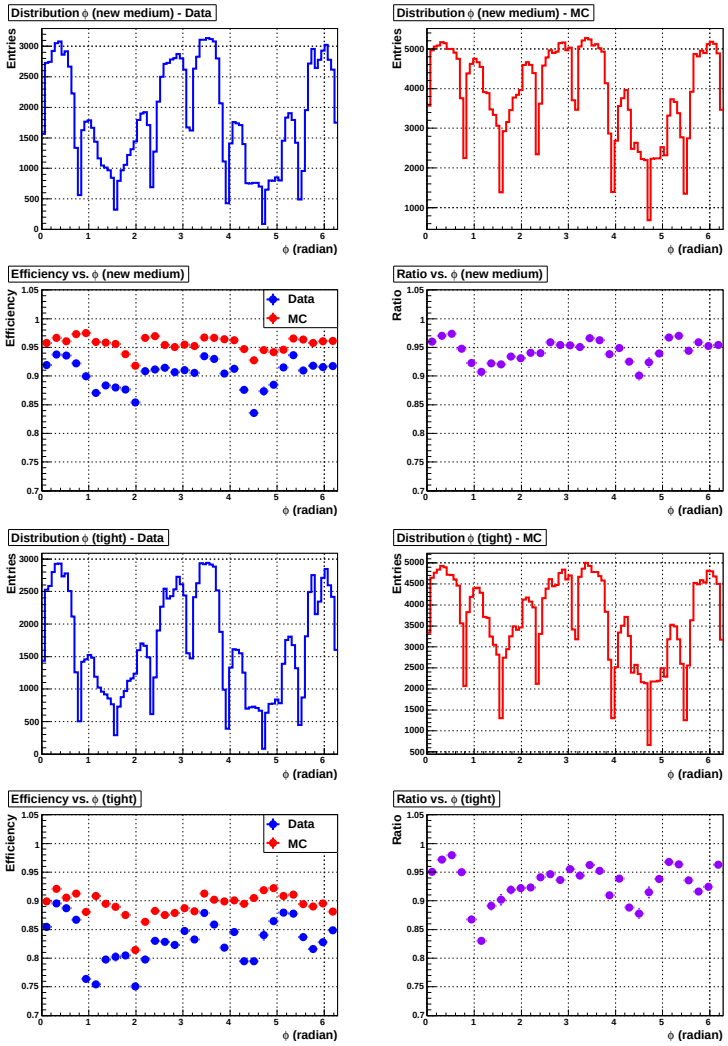

Figure 14: The distributions in φ for tracks passing tracknewmedium for data **(top left)** and MC **(top right)**, their efficiencies versus φ **(2nd left)**, and the data/MC ratio versus φ **(2nd right)**. The same four plots are also shown passing tracktight.

Source of systematic	trackloose	trackmedium	tracknewmedium	tracktight
tag-and-probe bias	0.3 %	0.3 %	0.3 %	0.3 %
background and cut variations	0.5 %	0.5 %	0.5 %	0.5 %
luminosity bias	–	–	–	–
simulation of beam along z	0.8 %	0.8 %	0.8 %	0.7 %
jet multiplicity (0 jets)	0.1 %	0.3 %	0.1 %	0.1 %
jet multiplicity (1 jet)	0.1 %	0.3 %	0.1 %	0.1 %
jet multiplicity (2 jets)	0.2 %	0.9 %	0.2 %	0.5 %
jet multiplicity (3+ jets)	0.3 %	1.4 %	0.3 %	0.8 %
statistical (V + jets)	0.1 %	0.1 %	0.1 %	0.1 %
statistical (other processes)	0.2 %	0.2 %	0.2 %	0.2 %
Total w/o statistical (2 jets)	1.0 %	1.3 %	1.0 %	1.0 %
Total (other processes) (2 jets)	**1.0 %**	**1.4 %**	**1.0 %**	**1.1 %**
time average, up to	*0.2 %*	*0.2 %*	*0.2 %*	*1.0 %*
average over φ, up to	*0.5 %*	*0.7 %*	*0.6 %*	*1.0 %*

Table 6: Summary of systematic uncertainties on tracking efficiency data/MC scale factors. For a typical physics analysis all systematic uncertainties including the one from limited Z-sample statistics are applicable. The uncertainty due to limited statistics is uniformly taken as 0.1 % for all V + jets processes, whereas 0.2 % is conservatively assumed for all other processes, which may sample the bins (and thus statistical uncertainties) with a different frequency. The uncertainty due to a shorter time period of the Summer 2009 Extended dataset and due to tracking efficiency variations in φ may be applicable for some analyses (both in italic). For details see text.

8 Prompt Muon Isolation Efficiency

This section addresses the isolation efficiency of prompt muons from electroweak processes. After introducing the principle of isolation efficiency estimation using the tag-and-probe method, we show those figures for data as measured on our $Z \to \mu^+\mu^-$ sample in data. Consecutively, we review the application of data/MC SFs using the CAFe framework, summarise the efficiencies and SFs, and discuss the systematic uncertainties on our SF measurements.

8.1 Principle of Efficiency Estimation

The efficiency of prompt muons to pass isolation requirements was measured using a $Z \to \mu^+\mu^-$ sample in data and $Z \to \mu^+\mu^-$ MC defined in Section 4 with a tag-and-probe method. The following, we describe this tag-and-probe selection. The track and muon identification criteria are the *same* for the tag and the probe muon:

- loose muon identification quality;
- Match between the muon segments and a track;
- trackloose track identification;
- Transverse momentum of the muon track of $p_{\mathrm{T}} > 15\,\mathrm{GeV}$;
- Local momentum of the muon as measured by the muon system only of $p_{\mathrm{T}} > 8\,\mathrm{GeV}$;
- Small transverse impact parameter d_0 (dca) with respect to the beamline for the muon track:
  - Tracks with SMT hits: $d_0 < 0.04\,\mathrm{cm}$;
  - Tracks without SMT hits: $d_0 < 0.2\,\mathrm{cm}$;
- Small difference of longitudinal impact parameters of the two muons: $\Delta(z_0^{\mu_1}, z_0^{\mu_2}) < 2\,\mathrm{cm}$;
- Acollinearity $\mathcal{A} \equiv \pi - |\varphi_{\mu_1} - \varphi_{\mu_2}| + |\pi - \theta_{\mu_1} - \theta_{\mu_2}|$ of at least $\mathcal{A} > 0.05$;
- Consistence of the invariant mass of the dimuon system with the Z peak: $70\,\mathrm{GeV} < m_{\mu\mu} < 120\,\mathrm{GeV}$.

Additionally, isolation requirements are imposed on the *tag* muon only in order to suppress backgrounds from W + jets or QCD processes:

- $\mathcal{I}^{\mathrm{trk}}_{\Delta R<0.5} < 2.5\,\mathrm{GeV}$;
- $\mathcal{I}^{\mathrm{cal}}_{0.1<\Delta R<0.4} < 10\,\mathrm{GeV}$;

In the past, cuts of $\mathcal{I}^{\mathrm{trk}}_{\Delta R<0.5} < 3.5\,\mathrm{GeV}$ and $\mathcal{I}^{\mathrm{cal}}_{0.1<\Delta R<0.4} < 2.5\,\mathrm{GeV}$ have been used. Due to the correlation between the tag and the probe, this choice of cuts was biasing the efficiency measurement towards higher values, and also enhancing the dependence on instantaneous luminosity. This is mainly due to $\mathcal{I}^{\mathrm{cal}}_{0.1<\Delta R<0.4}$, which, in contrast to $\mathcal{I}^{\mathrm{trk}}_{\Delta R<0.5}$, has much smaller handle to determine whether the energy deposit comes from the same primary vertex or another interaction (cf. Subsection 8.2). Therefore, we tightened the cut on $\mathcal{I}^{\mathrm{trk}}_{\Delta R<0.5}$ and loosened the one on $\mathcal{I}^{\mathrm{cal}}_{0.1<\Delta R<0.4}$.

8.2 Prompt Muon Isolation Efficiency

Over the past couple of years, the Tevatron has been breaking new ground in terms of operating instantaneous luminosities. Therefore, we start this Subsection by reviewing the luminosity dependence of the basic isolation variables serving as input to posterior isolation working points. After that, the prompt muon isolation efficiency dependence of the isolation working points on various variables like muon p_{T}, $\Delta R(\mu,\,\text{closest jet})$, η_{CFT}, $\mathscr{L}$, the number of primary vertices in an event N_{PV}, and time as found in data is presented.

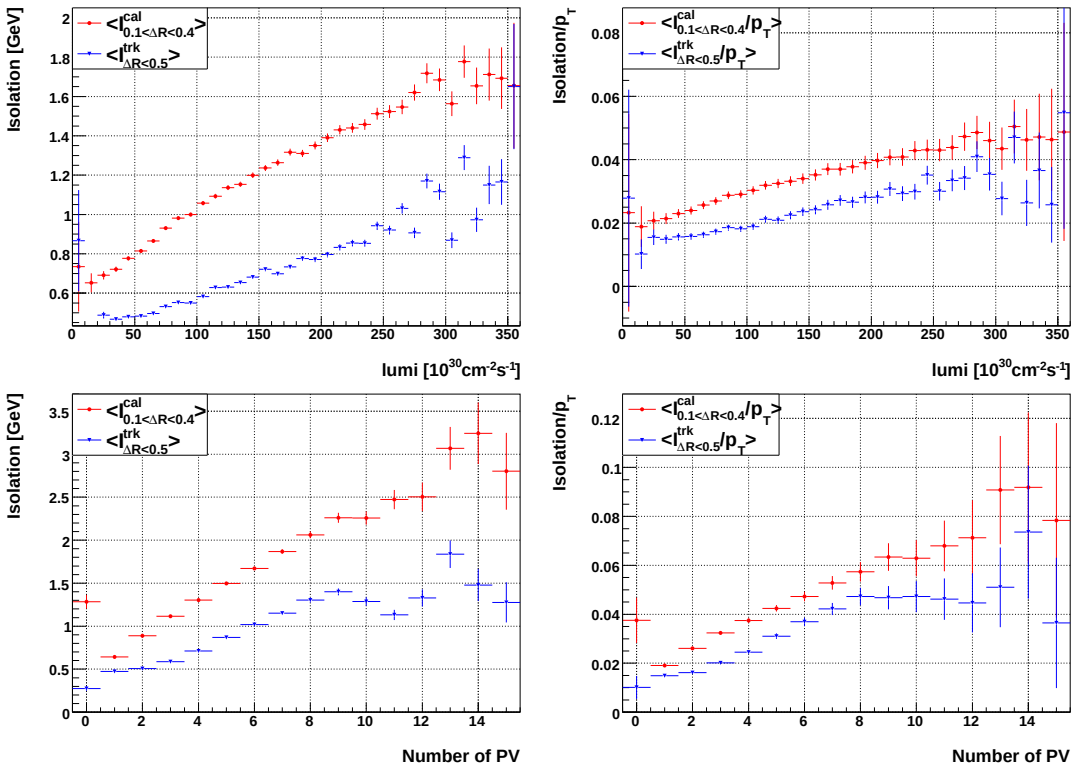

Figure 15: Isolation variables $\mathcal{I}^{\mathrm{cal}}_{0.1<\Delta R<0.4}$, $\mathcal{I}^{\mathrm{trk}}_{\Delta R<0.5}$ versus instantaneous luminosity $\mathscr{L}$ **(top left)** and the number of primary vertices in an event **(top right)**. The corresponding figures for p_{T}-scaled variables $\mathcal{I}^{\mathrm{cal}}_{0.1<\Delta R<0.4}/p_{\mathrm{T}}$ and $\mathcal{I}^{\mathrm{trk}}_{\Delta R<0.5}/p_{\mathrm{T}}$ are shown in the **(bottom left)** and **(bottom right)**, respectively.

Two basic input variables enter the definition of all working points for posterior isolation: $\mathcal{I}^{\mathrm{trk}}_{\Delta R<0.5}$ and $\mathcal{I}^{\mathrm{cal}}_{0.1<\Delta R<0.4}$ (cf. Section 3). The left column of Fig. 15 shows the dependence of their means $\langle\mathcal{I}^{\mathrm{trk}}_{\Delta R<0.5}\rangle_{\mathrm{bin}}$, $\langle\mathcal{I}^{\mathrm{cal}}_{0.1<\Delta R<0.4}\rangle_{\mathrm{bin}}$ on $\mathscr{L}$ and N_{PV}. Given the strong correlation between $\mathscr{L}$ and N_{PV}, the two plots are very similar. It is striking that $\mathcal{I}^{\mathrm{trk}}_{\Delta R<0.5}$ displays a notably smaller dependence on luminosity than $\mathcal{I}^{\mathrm{cal}}_{0.1<\Delta R<0.4}$. This is due to the fact that the sensitivity to any additional activity from other interactions in the same events is greatly reduced for $\mathcal{I}^{\mathrm{trk}}_{\Delta R<0.5}$: only tracks with $\Delta(z_0^{\mathrm{trk}},\,z_0^{\mu})<2\,\mathrm{cm}$ are allowed to enter its calculation. In contrast, no handles of this sort are used in the calculation of $\mathcal{I}^{\mathrm{cal}}_{0.1<\Delta R<0.4}$, and even if, they would be naturally much weaker. A qualitatively similar picture is found for $\langle\mathcal{I}^{\mathrm{trk}}_{\Delta R<0.5}/p^{\mu}_{\mathrm{T}}\rangle_{\mathrm{bin}}$, $\langle\mathcal{I}^{\mathrm{cal}}_{0.1<\Delta R<0.4}/p^{\mu}_{\mathrm{T}}\rangle_{\mathrm{bin}}$, shown in the right column of Fig. 15. In the long run, we plan to optimise the basic input variables $\mathcal{I}^{\mathrm{trk}}$, $\mathcal{I}^{\mathrm{cal}}$ in order to reduce their luminosity dependence.

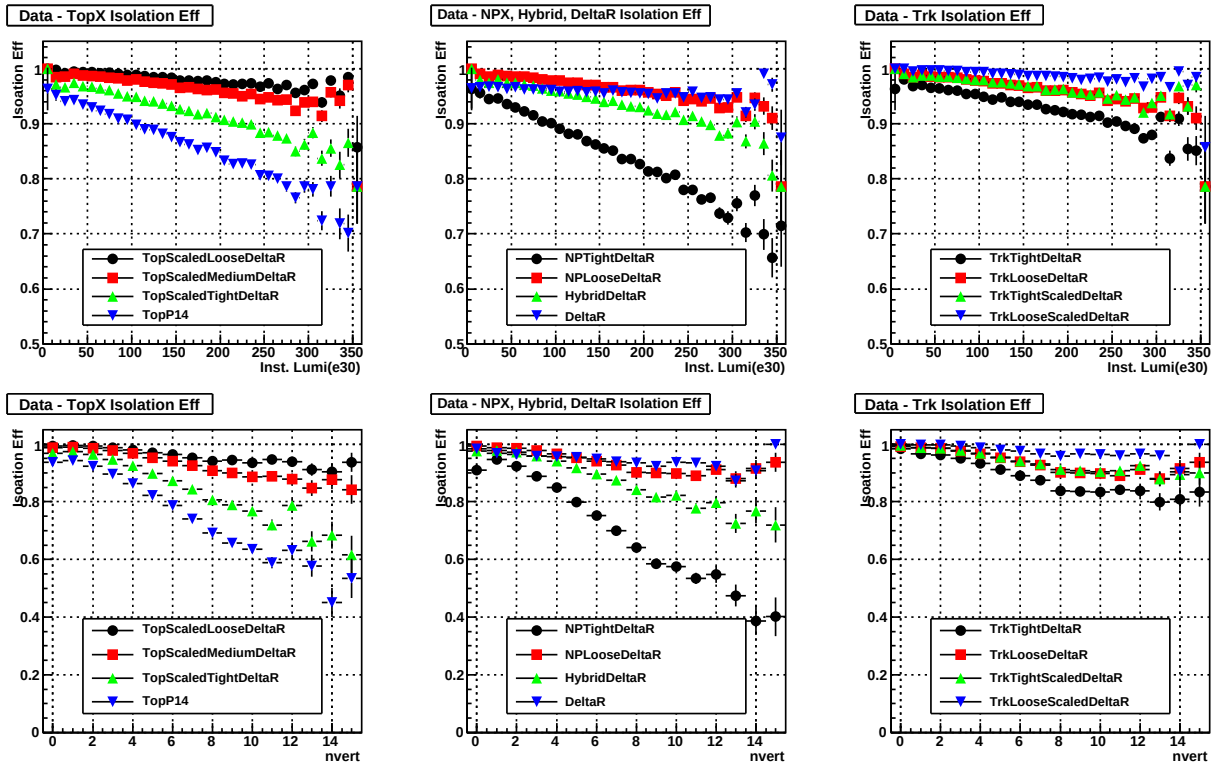

Figure 16: Efficiency of various isolation working points versus instantaneous luminosity $\mathscr{L}$ **(top row)** and the number of primary vertices N_{PV} **(bottom row)** in data. The figures are organised in "TopX" **(left column)**, "NPX" **(middle column)**, and "Trk" **(right column)** groups. All isolation efficiencies shown here except for deltaR are posterior, i.e. after the application of the $\Delta R(\mu, \text{closest jet}) > 0.5$ cut.

In the following, we show the isolation efficiency for prompt muons as measured in our $Z \to \mu^+\mu^-$ sample in data. We group the following working points together to be shown in the same plot:

"NPX" : deltaR, hybrid|deltaR, NPLoose|deltaR, NPTight|deltaR;

"TopX" : TopScaledLoose|deltaR, TopScaledMedium|deltaR, TopScaledTight|deltaR, TopP14|deltaR;

"Trk" : TrkLooseScaled|deltaR, TrkTightScaled|deltaR, TrkLoose|deltaR, TrkLoose|deltaR;

Keep in mind, that in the standard CAFe configuration the isolation cuts are applied in two steps: first, $\Delta R(\mu, \text{closest jet}) > 0.5$, and second the posterior isolation, like e.g. TrkTightScaled, which we generically denote as iso (cf. Subsection 8.3). Therefore, we show the posterior isolation under the condition that the deltaR requirement was passed, i.e. iso|deltaR.

Figure 16 shows the dependence of the prompt muon isolation efficiency on instantaneous luminosity $\mathscr{L}$ and the number of primary vertices in an event N_{PV}. A clear trend is evident: the tighter the isolation requirement, the stronger its susceptibility to pile up. TopP14|deltaR and NPTight|deltaR fare worst, losing about 30 % of their efficiency over the luminosity range shown. Given this dramatic luminosity dependence, we have designed new isolation variables

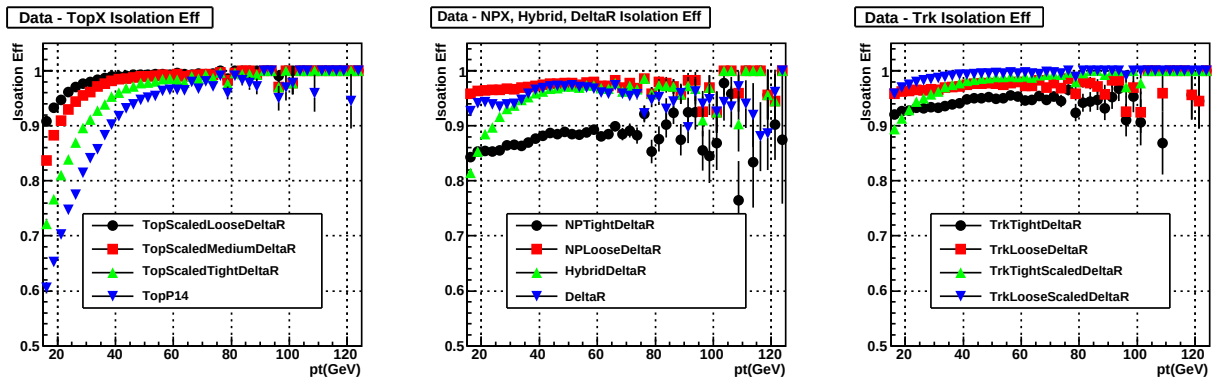

Figure 17: Efficiency of various isolation working points versus the muon p_{T} in data. The figures are organised in "TopX" **(left)**, "NPX" **(middle)**, and "Trk" **(right)** groups. All isolation efficiencies shown here except for deltaR are posterior, i.e. after the application of the $\Delta R(\mu, \text{closest jet}) > 0.5$ cut.

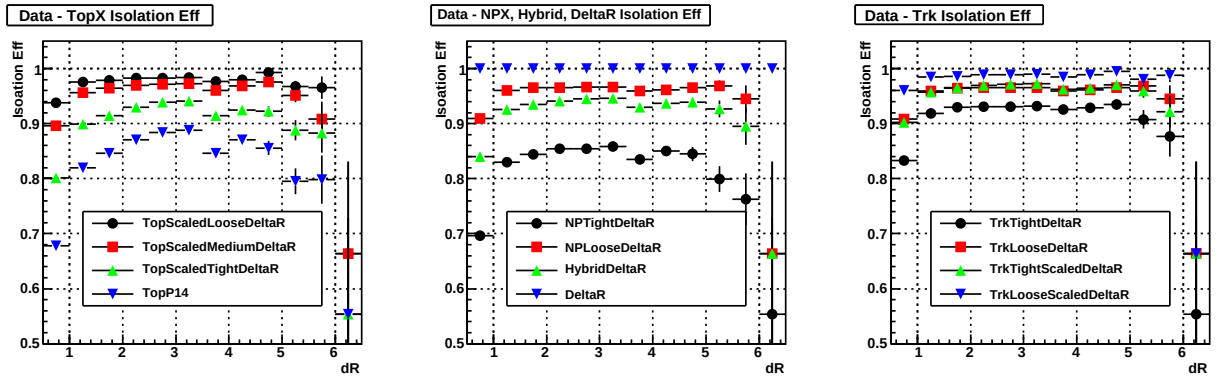

Figure 18: Efficiency of various isolation working points versus $\Delta R(\mu, \text{closest jet}) > 0.5$ in $\eta \times \varphi$ space in data. The figures are organised in "TopX" **(left)**, "NPX" **(middle)**, and "Trk" **(right)** groups. All isolation efficiencies shown here except for deltaR are posterior, i.e. after the application of the $\Delta R(\mu, \text{closest jet}) > 0.5$ cut.

which rely more strongly on track isolation rather than calorimeter isolation (the ones shown in the "Trk" group). Indeed, these new isolation variables show substantially better efficiency performance at high luminosity: TrkTightScaled|deltaR and TrkLoose|deltaR lose less than 10 % and less than 15 % of their efficiency, respectively. Comparing $1/p_{\mathrm{T}}$-scaled isolation variables with the corresponding "plain" ones which we believe to provide a similar rejection power against fakes, the former tend to perform better in terms of efficiency loss at high $\mathscr{L}$. The deltaR isolation shows very little dependence on instantaneous luminosity, as it is very unlikely that pile-up will form a jet with $E_{\mathrm{T}} > 15\,\mathrm{GeV}$.

The dependence of isolation efficiency on the transverse momentum of the muon is shown in Fig. 17. There is a striking difference in the shape of the efficiency curves for $1/p_{\mathrm{T}}$-scaled isolation variables compared to "plain" ones: while the former display a pronounced turn-on at low transverse momenta and asymptotically approach 100 % efficiency at high transverse momenta, the latter are rather flat in p_{T} and plateau at some efficiency $< 100\,\%$. Clearly, the behaviour of the $1/p_{\mathrm{T}}$-scaled isolation variables is much more favourable for a typical analysis

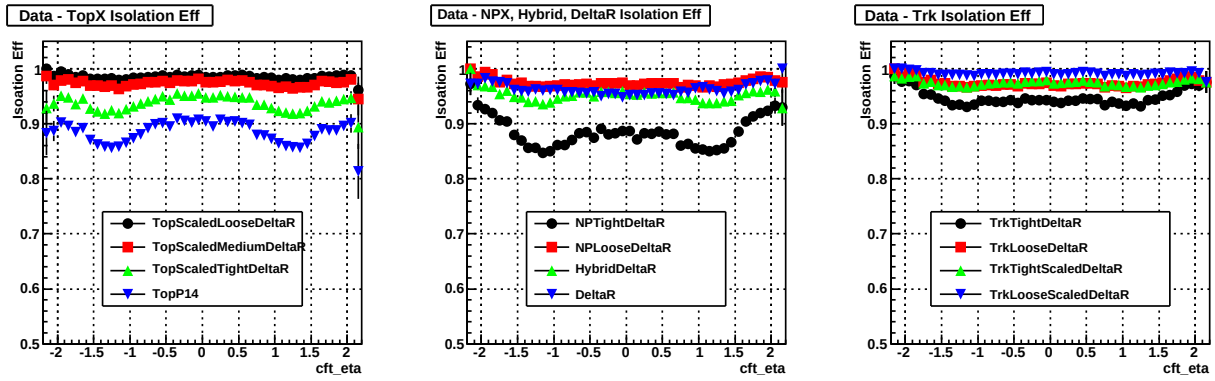

Figure 19: Efficiency of various isolation working points versus η_{CFT} in data. The figures are organised in "TopX" **(left)**, "NPX" **(middle)**, and "Trk" **(right)** groups. All isolation efficiencies shown here except for deltaR are posterior, i.e. after the application of the $\Delta R(\mu, \text{closest jet}) > 0.5$ cut.

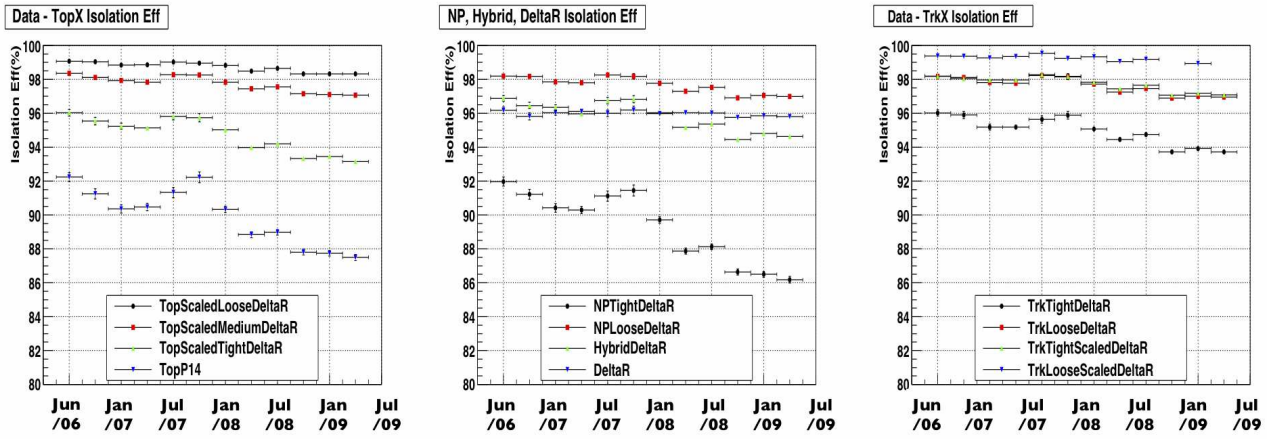

Figure 20: Efficiency of various isolation working points versus time in data. The figures are organised in "TopX" **(left)**, "NPX" **(middle)**, and "Trk" **(right)** groups. All isolation efficiencies shown here except for deltaR are posterior, i.e. after the application of the $\Delta R(\mu, \text{closest jet}) > 0.5$ cut.

interested in high-p_{T} muons from electroweak processes, as detailed in Subsection 3.4

Figure 18 displays the dependence of the isolation efficiency versus $\Delta R(\mu, \text{closest jet})$, i.e. the distance of the prompt muon candidate from the closest jet in the $\eta \times \varphi$ space. Because the $\Delta R(\mu, \text{closest jet})$ variable is defined only for events with 1 or more jets, the events with 0 jets are not shown in this Figure. This efficiency vs. ΔR distribution gives an insight into the isolation efficiency performance in a busy event with a lot of hadronic activity, like e.g. $V + nj$ where n is 2 or higher, or $t\bar{t}$ events. As a general trend, looser and $1/p_{\mathrm{T}}$-scaled isolation working points tend to provide a higher efficiency in dense hadronic environment. Again, isolation working points predominantly using track isolation tend to provide a somewhat better performance. Note that deltaR isolation efficiency is identical to unity in the $\Delta R > 0.5$ range shown by construction.

Naturally, isolation working points relying on calorimeter isolation depend crucially on the energy resolution of the calorimeter. Therefore, it is not surprising to find a somewhat decreased isolation efficiency in the region of the InterCryostat Detector (ICD), which covers

approximately $\eta_{\mathrm{CFT}} \in [1.0, 1.5]$. This is shown in Fig. 19. The drop in efficiency in the ICD region is much less pronounced for isolation working points predominantly using track isolation.

We investigated the performance of the isolation working points over time, which is documented in Fig. 20. Similar to the efficiency for track reconstruction, the isolation efficiency is sensitive to luminosity effects, and the drop in efficiency seen on that Figure is mostly due to the higher average luminosity over any given 3-month period.

8.3 Isolation Efficiency Data/MC Scale Factor Parametrisation

In the standard CAFe setup, the isolation is applied in two steps:

- Firstly, a cut on $\Delta R(\mu, \text{closest jet}) > 0.5$ is applied, i.e. the distance of the prompt muon candidate from the closest jet in the $\eta \times \varphi$ space should be greater than 0.5. This is the deltaR isolation requirement introduced in Subsection 3.4;
- Secondly, a *posterior* isolation requirement which we generally denote as iso, which can be one of the working points listed in Subsection 3.4.

Given the specifics of this setup, we certify data/MC SFs for the prompt muon isolation efficiency *only* for the deltaR working point, and the posterior isolation working points *under the condition*[8] that the deltaR requirement was fulfilled, i.e. iso|deltaR. In the CAFe framework, these data/MC SFs are applied using the `caf_eff_utils` package [8] to muons in simulated MC events in order to correct for any inaccuracy of its data description. The prompt muon isolation efficiencies are derived using the package `muid_eff` [14] for both data and MC. In the following, we describe these centrally certified data/MC SFs for deltaR and posterior isolation.

8.3.1 deltaR isolation

The deltaR isolation efficiency of prompt muons is moderately dependent on instantaneous luminosity, as can bee seen from Fig. 16. This dependence is somewhat different in data and simulated MC events, which necessitates a parametrisation of the data/MC SFs in $\mathscr{L}$. Moreover, it has been found that the luminosity effects are different in the central, ICD, and forward region due to detector specifications, as shown in Fig. 21. Ultimately, this will result in a different effect on the pseudorapidity distribution of muons in data and MC. Therefore, we choose to parametrise the data/MC SFs for deltaR isolation in $\mathscr{L} \times |\eta_{\mathrm{CFT}}|$. The binning is:

- in $\mathscr{L}$, 5 bins with boundaries of $\{0, 65, 100, 145, 190, \text{and } 300\,\mathrm{cm^{-2}s^{-1}}\}$ are used;
- in $|\eta_{\mathrm{CFT}}|$, 3 bins with boundaries of $\{0, 1.1, 1.5, 2.5\}$ are used.

The overall data/MC SF as measured using the procedure explained above is approximately 1.011.

[8] Therefore, the name "posterior" is used.

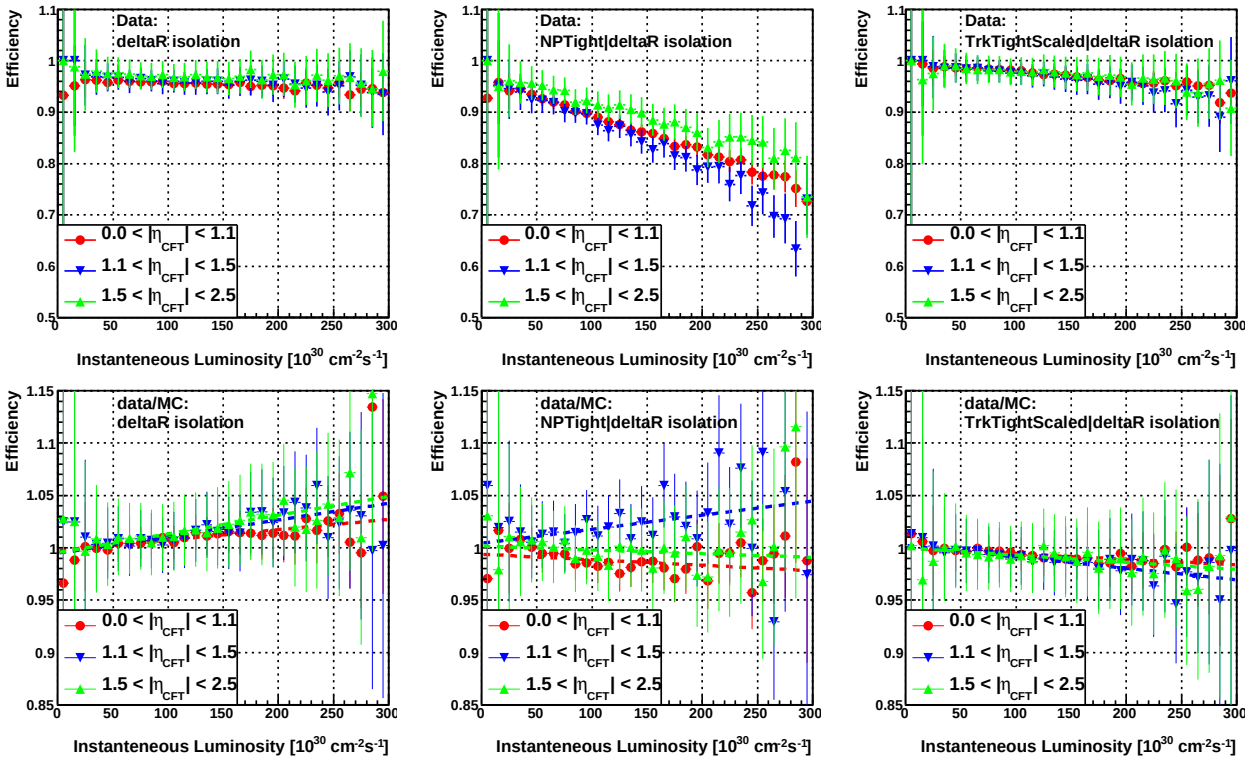

Figure 21: Isolation efficiency for prompt muons in data **(top row)** for the working points deltaR **(left column)**, NPTight|deltaR **(middle column)**, and TrkTightScaled|deltaR **(right column)**. The data/MC SFs are shown in respective order in the **bottom row**, together with a linear fit to each of the distributions.

8.3.2 Posterior isolation iso|deltaR

The *posterior* isolation efficiency iso|deltaR shows a luminosity dependence which can be quite notable for tight working points like NPTight|deltaR or TopP14|deltaR. The difference in the efficiency behaviour versus luminosity between the central, ICD, and forward region is typically much more pronounced for posterior isolation than for deltaR isolation discussed above. This is demonstrated for the most extreme example, NPTight, in Fig. 21. This difference is believed to come about due to modelling of the calorimeter response to minimum bias overlay data in MC. Naturally, this difference is almost not present in isolation working point relying more strongly on track isolation, of which TrkTightScaled|deltaR is shown in Fig. 21 as a typical example, and the difference of the SFs between the central, ICD, and forward region is small. Similarly to the deltaR case, this dependence requires an explicit parametrisation of the data/MC SFs in $|\eta_{\mathrm{CFT}}|$.

Due to Bremsstrahlung and other effects, the isolation efficiency for prompt muons can be dependent on the transverse momentum of the muon, as demonstrated in Fig. 17. Since there are some differences in the p_{T} dependence between data and MC, a parametrisation of SFs in the p_{T} of the muon is essential.

The decrease in the prompt muon isolation efficiency in proximity of neighbouring jets shown in Fig. 18 (for data only) is different between data and MC, and requires a parametrisation in

Statistical figure	TopScaledLoose	TopScaledMedium	TopScaledTight	TopP14	NPLoose	NPTight
Efficiency	98.4 %	97.3 %	93.8 %	88.4 %	97.2 %	87.5 %
Eff. (w/o $\mathscr{L}$ rew.)	98.7 %	97.7 %	94.6 %	89.7 %	97.6 %	89.0 %
Data/MC SF	0.994	0.993	0.992	0.990	0.991	0.990

Statistical figure	TrkLoose	TrkLoose	TrkLooseScaled	TrkTightScaled	hybrid	deltaR
Efficiency	97.2 %	94.2 %	99.0 %	97.3 %	95.0 %	95.9 %
Eff. (w/o $\mathscr{L}$ rew.)	97.6 %	94.9 %	99.2 %	97.7 %	95.7 %	94.1 %
Data/MC SF	0.990	0.987	0.995	0.991	0.991	1.011

Table 7: Figures for overall isolation efficiency for prompt muons, as well as data/MC SFs, as measured on our $Z \to \mu^+\mu^-$ sample in data. The numbers are shown for the deltaR isolation, and the posterior isolation criteria under the condition that deltaR was passed. The statistical uncertainties for all the values can be uniformly assumed at the 0.1 % level. For details see text.

$\Delta R(\mu, \text{closest jet})$.

We parametrise the data/MC SFs for prompt muon isolation efficiency in $|\eta_{\text{CFT}}| \times p_{\text{T}} \times \Delta R$. Given that these are already three variables and regarding that the number of the parametrisation points rises with the power of the number of parametrisation variables, an explicit dependence on instantaneous luminosity cannot be included as a fourth fully-correlated parameter. On the other hand, the luminosity dependence cannot be factorised due to its correlation with the other three variables. Therefore, we do not include it, but rely on our luminosity reweighting procedure introduced in this certification round and described in Section 5. We choose the following binning to parametrise data/MC SFs for posterior isolation efficiency:

- in $|\eta_{\text{CFT}}|$, 3 bins with boundaries of $\{0, 1.1, 1.5, 2.5\}$ are used;
- in p_{T}, 4 bins with boundaries of $\{15, 25, 35, 45, 125\,\text{GeV}\}$ are defined;
- in $\Delta R(\mu, \text{closest jet})$, we use 5 bins with boundaries of $\{0, 0.5, 1, 2.5, 10, 100\}$, where the last bins contains all $Z \to \mu^+\mu^-$ events without any additional jets with $p_{\text{T}} > 15\,\text{GeV}$.

The overall data/MC SF as measured using the procedure explained above are typically slightly below unity, and are summarised in Table 7 in the next Subsection.

8.4 Overall Isolation Efficiency and Data/MC Scale Factors for Prompt Muons

In Table 7, the overall isolation efficiency for prompt muons, as measured on our $Z \to \mu^+\mu^-$ sample in data, is given. The efficiencies are shown for the deltaR isolation, and the posterior isolation criteria under the condition that deltaR was passed, i.e. isolation|deltaR. For comparison, the same figures are given before luminosity reweighting to the `2MUhighpt` skim spectrum. Further, the overall data/MC SFs are presented. All these overall results depend on the topology in $\eta \times \varphi$ and other variables, so are only indicative.

The prompt muon isolation efficiencies stored in the SPC files as measured in this certification round (i.e. `v05-01-02` of `muid_eff`) can be found at [18].

8.5 Systematic Uncertainty Isolation Efficiency Data/MC Scale Factors

As detailed in Subsection 8.3, the isolation requirerements of $\Delta R(\mu, \text{closest jet}) > 0.5$ and the posterior isolation like e.g. TrkTightScaled are applied after each other to a prompt muon candidate. Therefore, any possible systematic biases can be categorised in two groups:

- systematic biases which will affect deltaR and the posterior isolation in the same way. These biases will be fully correlated, and are therefore to be accounted for only once;
- systematic biases which will affect *either* deltaR isolation *or* the posterior isolation. Typically, these biases are due to not explicitly accounting for the dependence of the data/MC SFs on a variable, like e.g. $\mathscr{L}$ for posterior isolation. Clearly, such biases have to be accounted for only for the respective isolation criterion.

In the following, we quantitatively assess the magnitude of these possible biases. Unless explicitly stated otherwise, these biases belong to the first category above.

8.5.1 Tag-and-Probe Biases

There are three inherent sources for potential biases in the tag-and-probe method: firstly, biases of the method per se, secondly, biases due to correlations between the tag and the probe in the offline or in the trigger selection. We address them separately:

- Existence of a possible per se bias in the method has been quantitatively assessed in [17] (`p14-pass1`) by looking at the difference between the tag and probe measurements and the genuine efficiency in MC events. The bias is found to be 0.2 %. The study has not been repeated within `p20`, but the results are thought to remain valid.
- A possible systematic bias due to correlations between the tag and the probe due to offline selection criteria on the probe was estimated by reverting to the isolation cuts on the probe used in the previous certification rounds, that is $\mathcal{I}^{\text{cal}}_{0.1<\Delta R<0.4} < 2.5\,\text{GeV}$ in addition to $\mathcal{I}^{\text{trk}}_{\Delta R<0.5} < 2.5\,\text{GeV}$. Doing this, we observe a variation in the data/MC SFs at the 0.2 % level.
- We have studied the correlation between the trigger requirement on the tag and the isolation efficiency of the probe by comparing the data/MC SF variation between the `MUHI`x, $x =$ `1`, `2`, `3` trigger families which we use to derive the efficiencies, and the `MUHI1` trigger family. The main difference between the two is that `MUHI1` triggers do not require any isolation at L1, whereas `MUHI`x, $x =$ `2`, `3` do. We find this difference to be below the 0.1 % level and thus negligible. The reason to use `MUHI`x, $x =$ `1`, `2`, `3` for the SF derivation is more statistics at $\mathscr{L} > 200\,\text{cm}^{-2}\text{s}^{-1}$, where `MUHI1` is highly prescaled.

Based on the studies above, we assign an overall systematic uncertainty of $0.2\,\% \oplus 0.2\,\% = 0.3\,\%$ due to possible tag-and-probe biases.

8.5.2 Background Contamination

Clearly, a contamination of our $Z \to \mu^+\mu^-$ sample with non-prompt muons like e.g. muons from heavy flavour quark decays will bias downwards our efficiency measurement in data. We estimate a possible bias due to this contamination by tightening the cuts on the dimuon mass of the $Z \to \mu^+\mu^-$ candidate events to $80\,\text{GeV} < m_{\mu\mu} < 100\,\text{GeV}$ and $85\,\text{GeV} < m_{\mu\mu} < 95\,\text{GeV}$, which results in a variation of the measured efficiency by about 0.1 % and 0.2 %, respectively. Thus, we conservatively quote a systematic uncertainty of 0.2 % due to a possible background contamination.

8.5.3 Correlation with Muon Quality Requirements

As detailed in Subsection 3.5, we assume that the separate measurements of efficiencies for muon identification, track identification, and the isolation of prompt muons are independent and thus factorisable. However, there may be some correlations between the three. We assess the systematic uncertainties due to possible correlation between isolation requirements and the muon quality working points by evaluating the variation in data/MC SFs between the loose and mediumnseg3 requirements. We find variations of up to 0.1 %, which we quote as a systematic uncertainty.

8.5.4 Correlation with Track Quality Requirements

Similarly to the correlation with muon identification working points in the previous Subsection, we evaluate the systematic uncertainty due to possible correlations between isolation and track quality requirements by studying the variation in data/MC SFs between the trackloose and tracktight working points. Again, we find variations of up to 0.1 %, which we quote as a systematic uncertainty.

8.5.5 Instantaneous Luminosity Dependence

The isolation efficiency shows a pronounced dependence on the instantaneous luminosity $\mathscr{L}$, which is mostly due to hadronic energy deposition in the detector and tracks from pile-up at high luminosities. However, the luminosity spectrum found in the MC sample used for the efficiency calculation is much softer (cf. Section 5) than in data. Moreover, the luminosity spectrum in data is biased by the specific choice of (mostly prescaled) triggers. Therefore, it is necessary to reweight the luminosity profile in data and in MC to the profile found in the `2Mhighpt` skim.

Figure 21 shows the track detection efficiency versus luminosity in data and MC for the deltaR quality. Clearly, the dependence is rather different for data and MC, which necessitates the parametrisation of the tracking efficiency SFs in luminosity. Owing to this explicit parametrisation, there is no systematic uncertainty due to the luminosity spectrum. The same Figure shows a similar dependence for the NPTight|deltaR isolation. However, because the posterior isolation is not parametrised in luminosity for reasons detailed in Subsection 8.3, there is a resulting systematic uncertainty. To quantify it, we take a representative analysis, in this case a $t\bar{t}$ selection in the $\mu + 4$ jets final states before any b-tag requirement [16], and extract the luminosity profile found in data and in the $t\bar{t}$ MC signal. We reweight the data

and MC of our $Z \to \mu^+\mu^-$ selection to these respective luminosity profiles, and investigate the change of the SFs for the posterior isolation. This results in systematic uncertainties of up to 0.8 % (NPTight|deltaR). The uncertainties for each individual posterior isolation requirement are given in Table 8. Certainly, this somewhat conservative procedure does not yield a precise estimate for any given analysis, however it serves as a good indication about the possible magnitude of systematic biases which could be expected.

8.5.6 Limited Z-sample Statistics

The limited size of our Z-sample in data and MC results in a statistical uncertainty on the data/MC SF. For data, it amounts up to 0.06 % for the tightest requirements TopP14 and NPTight. The corresponding values for MC are well below data due to a larger sample size. Across all isolation quality requirements, we uniformly quote an uncertainty of 0.1% on the data/MC SFs due to limited statistics.

Note, that the above SF uncertainty is valid only for V + jets processes, whereas an uncertainty of 0.2 % should be conservatively assumed for all other processes, which may sample the SF bins (and thus statistical uncertainties) with a different frequency.

As of `p21-br-16` of the `caf_eff_util` package it is possible to access the statistical uncertainties in CAFe on an event-by-event basis via the `stat` processor. Some analyses may choose to use this approach rather than a flat uncertainty we centrally provide.

8.5.7 Trigger Version / Time Dependence

All isolation cuts have a negligible dependence on the trigger version. Figure 20 shows the isolation efficiency for prompt muons versus time. A clear variation can be observed, which can be mostly attributed to changes in average instantaneous luminosity over that time period. However, it is possible that the data/MC overall SF could change by up to 1 % due to e.g. dead SMT modules or ageing of the CFT fibres in case if only a particular subset of the Summer 2009 Extended dataset is analysed. We do not assign an explicit systematic uncertainty due to this, however we would like to make the analysers aware of this fact if they investigate only a fraction of the certified dataset.

8.5.8 Systematics Summary

The uncertainties on data/MC isolation efficiency scale factors due to possible systematic biases discussed above are summarized in Table 6. Please keep in mind that the data/MC SFs are applied twice: for deltaR isolation, and consecutively for the particular posterior isolation working point (under the condition that deltaR was passed), i.e. isolation|deltaR. Since the method and also the selection for measuring the isolation efficiency is exactly the same for deltaR and posterior isolation, the systematic uncertainties due to tag-and-probe, backgrounds, correlations to muon or track ID, and limited Z-sample statistics can be taken as fully correlated, whereas the systematic uncertainty due to missing luminosity parametrisation is applicable to posterior isolation only. Thus, for a typical physics analysis, the total systematic uncertainty on the prompt muon isolation efficiency like e.g. TrkTightScaled will be the Gaussian sum of all systematic uncertainties for deltaR isolation, and the systematic uncertainty due to missing luminosity parametrisation for TrkTightScaled|deltaR isolation, i.e. $0.4\,\% \oplus 0.3\,\% = 0.5\,\%$.

Source of systematic	TopScaledLoose	TopScaledMedium	TopScaledTight	TopP14	NPLoose	NPTight
tag-and-probe	0.3 %	0.3 %	0.3 %	0.3 %	0.3 %	0.3 %
backgrounds	0.2 %	0.2 %	0.2 %	0.2 %	0.2 %	0.2 %
correlation to muon ID	0.1 %	0.1 %	0.1 %	0.1 %	0.1 %	0.1 %
correlation to track ID	0.1 %	0.1 %	0.1 %	0.1 %	0.1 %	0.1 %
luminosity	0.1 %	0.2 %	0.4 %	0.7 %	0.2 %	0.8 %
statistical (V + jets)	0.1 %	0.1 %	0.1 %	0.1 %	0.1 %	0.1 %
statistical (other processes)	0.2 %	0.2 %	0.2 %	0.2 %	0.2 %	0.2 %
Total w/o statistical	0.4 %	0.4 %	0.6 %	0.8 %	0.4 %	0.9 %
Total (other processes)	**0.4 %**	0.5 **%**	**0.6 %**	**0.8 %**	**0.5 %**	**0.9 %**
time average, up to	*1.0 %*	*1.0 %*	*1.0 %*	*1.0 %*	*1.0 %*	*1.0 %*

Source of systematic	TrkLoose	TrkLoose	TrkLooseScaled	TrkTightScaled	hybrid	deltaR
tag-and-probe	0.3 %	0.3 %	0.3 %	0.3 %	0.3 %	0.3 %
backgrounds	0.2 %	0.2 %	0.2 %	0.2 %	0.2 %	0.2 %
correlation to muon ID	0.1 %	0.1 %	0.1 %	0.1 %	0.1 %	0.1 %
correlation to track ID	0.1 %	0.1 %	0.1 %	0.1 %	0.1 %	0.1 %
luminosity	0.2 %	0.4 %	0.1 %	0.2 %	0.3 %	−−
statistical (V + jets)	0.1 %	0.1 %	0.1 %	0.1 %	0.1 %	0.1 %
statistical (other processes)	0.2 %	0.2 %	0.2 %	0.2 %	0.2 %	0.2 %
Total w/o statistical	0.4 %	0.6 %	0.4 %	0.4 %	0.5 %	0.4 %
Total (other processes)	**0.5 %**	0.6 **%**	**0.4 %**	**0.5 %**	**0.5 %**	**0.4 %**
time average, up to	*1.0 %*	*1.0 %*	*1.0 %*	*1.0 %*	*1.0 %*	*1.0 %*

Table 8: Summary of systematic uncertainties on prompt muon isolation efficiency data/MC scale factors. For a typical physics analysis all systematic uncertainties including the one from limited Z-sample statistics are applicable. The uncertainty due to limited statistics is uniformly taken as 0.1 % for all V + jets processes, whereas 0.2 % is conservatively assumed for all other processes, which may sample the bins (and thus statistical uncertainties) with a different frequency. The uncertainty due to a shorter time period of the Summer 2009 Extended dataset may be applicable for some analyses (shown in italic). Beware that deltaR isolation and posterior isolation requirements are applied independently, and that most of their systematic uncertainties are fully correlated. See text for details.

9 Conclusion

The efficiency for identification and reconstruction of prompt muons with the muon spectrometer and central tracker of the D0 detector, as measured in a $Z \to \mu^+\mu^-$ sample in the Summer 2009 Extended dataset of 4.2 fb^{-1}, is presented. New operating points for the identification and reconstruction of prompt muons are defined in order to better cope with higher instantaneous luminosities and adverse detector ageing effects. Where necessary, references to their usage utilising the standard DØ `V+jets` and CAFE framework are given. The resulting data/MC corrections are derived and presented for Monte Carlo events simulated with release `p20.09.xx` of the D0 software. The main changes and improvements with respect to the previous determinations of prompt muon identification and reconstruction efficiencies in `p17` and `p20`, as documented in Refs. [1, 2], are summarised.

This certification round is the result of more than half a year of hard work of the Muon Identification and Algorithms group in 2009-2010, and has lead to a substantially better understanding of various aspects of muon reconstruction, among others the ultimate resolution of the long-standing "η-horns" problem.

The experimental techniques and procedures used to determine the identification and reconstruction efficiencies of prompt muons presented in this technical memo note are identical to those used for the full 9.7 fb^{-1} dataset collected by the D0 experiment during Run II of Fermilab's Tevatron $p\bar{p}$ Collider, and thus of general nature.

References

[1] P. Calfayan *et al.* for the DØ Muon ID group, "Muon Identification Certification for `p17` Data", DØ note 5175, February 2007.

[2] S. Cho *et al.* for the DØ Muon ID group, "Muon Identification Certification for `p20` Data", DØ note 5824, December 2008.

[3] D. Hedin, "Run IIb Local Muon Momentum Resolution", DØ note 5998, October 2009.

[4] M. Arthaud, F. Deliot, B. Tuchming, V. Sharyy, D. Vilanova, DØ Note 5449, "Muon Momentum Oversmearing for `p20` Data", 2007.

[5] O. Brandt, D. Hedin, A.S. Santos and B. Tuchming for the DØ Muon ID group, "The Muon Momentum Resolution fo the D0 Experiment in Run II", FERMILAB-TM-2540-PPD, DØ Note 6190, 2011.

[6] D. Hedin, "Preliminary D0 Punchthrough Rates", DØ note 1738, 1993.

[7] `MuonSelector` documentation:
http://www-d0.fnal.gov/d0dist/dist/releases/development/caf_util/doc/html/classcaf__util_1_1MuonSelector.html.

[8] Documentation for correcting the MC efficiencies within CAF using `caf_eff_utils`:
http://www-d0.fnal.gov/d0dist/dist/releases/development/caf_eff_utils/doc/html/.

[9] Documentation for computation of trigger efficiencies within CAF `caf_trigger`:
http://www-d0.fnal.gov/d0dist/dist/releases/development/caf_trigger/doc/readme.html.

[10] Gavin Hesketh for the DØ Muon Algorithm and Identification groups, "Content of the `p17` Muon Thumbnail", DØ note 4735.

[11] S. Chevalier-Théry , F. Déliot , B. Tuchming, "Scintillator Timing Studies For Muon Identification", DØ note 5861, 2009.

[12] S. Chevalier-Théry , U. Bassler , F. Déliot , B. Tuchming, "Track Chi2 Cut Studies For Muon Identification", DØ note 5996, 2009.

[13] D. Hedin, talk given in the muon ID group meeting on 9/1/2009,
http://www-d0.hef.kun.nl//fullAgenda.php?ida=a091348.

[14] `muid_eff` package to compute and store muon related efficiencies:
https://plone4.fnal.gov/P1/D0Wiki/object-id/mu_id/muid_eff/.

[15] `wzreco` and `muo_cert` documents:
https://plone4.fnal.gov/P1/D0Wiki/object-id/mu_id/muo_cert/
http://www-d0.fnal.gov/d0dist/dist/releases/development/wzreco/doc
http://www-d0.fnal.gov/d0dist/dist/releases/development/muo_cert/doc

[16] O. Brandt *et al.*, "Measurement of the $t\bar{t}$ Cross Section in the lepton+jets Channel Using $5.3\,\mathrm{fb}^{-1}$", DØ Note XXXX.

[17] F. Déliot, G. Hesketh, P. Telford, B. Tuchming, DØ Note 4749, "Measurement of $\sigma(p\bar{p} \to WX) \times \mathrm{Br}(W \to \mu\nu)$ at $\sqrt{s} = 1.96$ TeV".

[18] Full set of certification control plots for `v05-01-02` of `muid_eff` can be found at:
http://www-clued0.fnal.gov/ obrandt/d0_private/muonID_certification/v05-01-02/control_data.ps
http://www-clued0.fnal.gov/ obrandt/d0_private/muonID_certification/v05-01-02/control_mc.ps